NASA CR-65586

FINAL REPORT

THE FLAW GROWTH CHARACTERISTICS OF 6Al-4V TITANIUM USED IN APOLLO SPACECRAFT PRESSURE VESSELS

By

C. F. Tiffany & J. N. Masters

Prepared for

NATIONAL AERONAUTICS & SPACE ADMINISTRATION

March 1967

Contract NAS 9-6665

Technical Management

NASA Manned Spaceflight Center

Houston, Texas

S. V. Glorioso

Aerospace Group
THE BOEING COMPANY

Seattle, Washington

FOREWORD

The failure of two Apollo Spacecraft Propulsion System (SPS) fuel tanks during 1966 while pressure testing with methanol prompted NASA/Manned Spacecraft Center, Houston, Texas, to initiate a study aimed at obtaining laboratory verification of the cause of the tank failures and obtaining a quantitative evaluation of the expected performance of the other various Apollo tanks in their test and service environments. As part of this study NASA requested The Space Division of The Boeing Company to perform an investigation of the flaw growth characteristics of the 6Al-4V titanium tankage material. This work was performed under NASA Contract NAS 9-6665 during the period from November 9, 1966 to February 17, 1967 and the results are reported herein. The work was administered under the direction of Mr. S. V. Glorioso at NASA/MSC.

Boeing personnel who participated in the investigation include C. F. Tiffany, Program Supervisor, J. N. Masters, Technical Leader, and P. M. Lorenz, research engineer. Structural testing of specimens was conducted by A. A. Ottlyk and G. E VanStaalduine. Metallurgical support was provided by R. E. Regan.

The information contained in this document is also released as Boeing Document D2-113530-1.

THE FLAW GROWTH CHARACTERISTICS OF 6Al-4V TITANIUM USED IN APOLLO SPACECRAFT PRESSURE VESSELS

By

C. F. Tiffany & J. N. Masters

ABSTRACT

Plane-strain cyclic and sustained load flaw growth characteristics were evaluated for 6Al-4V titanium forgings and weldment heat affected zones. Investigations were conducted at temperatures ranging from 65°F to 110°F in the environments of Aerozene 50, monomethylhydrazene, nitrogen tetroxide, methanol, Freon MF, and distilled water (with and without sodium chromate additions). Basis for evaluation was the determination of threshold stress intensity values (that K_I value below which sustained load flaw growth would not occur) in the various liquid environments. Data generated in this report are presented in a manner which is directly useful in establishing design, inspection, testing, and operational requirements of Apollo, as well as other pressure vessels.

CONTENTS

yDJ.

ILLUSTRATIONS

ILLUSTRATIONS (Continued)

TABLES

SUMMARY

The objective of this investigation was to determine plane-strain subcritical flaw growth characteristics for forged and welded 6Al-4V titanium. Tests were conducted on uniaxially loaded precracked surface flawed specimens in the following environments:

TEST FLUID	TEST TEMPERATURE °F
Aerozene 50	70 & 110
Monomethylhydrazene	105
Nitrogen Tetroxide - Inhibited	70, 85, & 105
Methanol	72
Freon MF	65 & 85
Distilled Water	65
Inhibited Distilled Water (500 PPM Sodium Chromate)	72

Sustained load threshold stress intensity values were obtained for each of the above environments. In addition, limited cyclic tests were performed in Aerozene 50, Freon MF, distilled water, and inhibited distilled water.

The results of this test program showed that sustained load threshold values (in terms of initial-to-critical stress intensity ratios) are relatively high, exceeding 75%, with the exception of three environments: methanol, Freon MF, and at test temperatures exceeding 85°F, nitrogen tetroxide. Little or no difference in sustained load behavior was observed between base metal and weld heat affected zone (HAZ) except in the environment of Freon MF. In this case the flaw growth was significantly more pronounced in the HAZ than in base metal. At stress intensity levels below the sustained load threshold value, cyclic load flaw growth rates are quite low, and are not considered to be a serious problem.

For the case of methanol, the base metal threshold value is 24 percent of the critical stress intensity (K_{Ic}). With regard to the failed SPS fuel tanks, this value indicates that initial flaws as small as about 0.003 inches deep could have grown to failure when exposed to methanol at maximum operating stress.

1.0 INTRODUCTION

Life prediction of pressure vessels subjected to cyclic or extended time service requirements requires knowledge of:

1) The flaw size which will cause immediate failure upon application of operating pressure (i.e., the critical flaw size);

2) The initial flaw sizes existing in the vessel prior to being placed into service, and;

3) Conditions under which the initial flaws can grow to critical size during the desired life of the vessel.

Information required in items 1) and 3) above can be developed through laboratory testing of preflawed specimens. By using linear elastic fracture mechanics procedures, the generated data can then be used to define the item 2) requirements; that is,

1) What are the allowable initial flaw sizes?

2) What are the nondestructive inspection or proof test requirements?

3) If necessary, what service limitations should be imposed on the vessel?

The investigation reported herein was undertaken to generate the required experimental data on 6Al-4V forgings and weldments in environments of several storeable propellants and vessel test fluids of current interest.

2.0 BACKGROUND

Vessel service performance is dependent upon the critical flaw size, the maximum initial flaw size existing when the vessel is placed into service, and the subcritical flaw growth characteristics of the vessel materials. Critical flaw sizes, in turn, are dependent upon the fracture toughness, applied stress, and, in the case of thin walled vessels, the wall thickness. Estimates of actual initial flaw sizes can be made by nondestructive testing, or with knowledge gained during proof testing[1]. Growth of these initial flaws can result from cyclic loading, sustained stress loading, or combinations of both. Several papers are available, References (1) through (4), which provide detailed discussions of these facets. The following paragraphs are presented to summarize those aspects which have particular application to the present program:

2.1 CRITICAL FLAW SIZES

Figure 1 schematically relates stress and flaw size for a given material and for the condition of a small flaw in a large body (i.e., thick wall) loaded in tension. If the operating stress is σ, then the corresponding flaw size that would cause fracture at that stress is noted as $(a/Q)_{cr}$. Assuming that the structure is known to contain an initial flaw of $(a/Q)_i$, the growth of the initial flaw would result in failure when its size reached the value of $(a/Q)_{cr}$. For this case of small flaws in thick structure, complete fracture and possible shattering of the vessel could be expected. On the other hand, if the material fracture toughness (K_{Ic}) is sufficiently high or the operating stress is sufficiently low, it is possible that the calculated critical flaw size significantly exceeds the wall thickness of the vessel. In such a case, if growth occurs, the initial flaw would be expected to grow through the thickness and the vessel would leak rather than fail catastrophically.

In order to accurately predict the failure mode of a pressure vessel as well as estimate its operational life, it is necessary to know the stress intensity for flaws which become very deep with respect to the wall thickness. The stress intensity solution for the semi-elliptical surface flaw shown in Figure 1 was derived by Irwin[5] and has been found to be reasonably accurate for flaw depths up to about 50 percent of the material thickness. At greater depths the applied stress intensity is magnified due to the effect of the free surface near the flaw tip. This means that in thin walled vessels (i.e., those vessels where the critical flaw size approaches or exceeds the wall thickness) the flaw tip stress intensity can attain the critical value (i.e., the K_{Ic} value) at a flaw size which is significantly smaller than that which would be predicted using the equation shown in Figure 1.

Kobayashi[6] and Smith[7] have developed solutions for deep surface flaws which are very long with respect to their depth (i.e., small a/2c values) and for semicircular surface flaws (i.e., a/2c = 0.5), respectively. The results are shown in terms of a stress intensity magnification factor, M_K, versus a/t in Figure 2. This factor is applied to the original Irwin equation to obtain the stress intensity for deep surface flaws. It is seen that the magnification reaches a maximum value of less than 10 percent for semicircular flaws, whereas an increase of about 60 percent is observed for flaws with smaller a/2c values. Experimental data obtained on several materials with varying flaw sizes and shapes appears to provide a fair degree of substantiation to the results of References 6 and 7 (see Reference 10).

To illustrate the effect of the deep flaw stress intensity magnification on predicted critical flaw sizes it is both convenient and safe to assume the vessel contains flaws which are long with respect to their depth. For these types of flaws the size can be described in terms of only the flaw depth, a, since the flaw shape parameter, Q, is approximately equal to unity. A predicted critical flaw size curve (obtained using Kobayashi's M_K curve) for a typical tank material and wall thickness is shown in Figure 3. For comparison the critical flaw size curve for the same material in a thick walled vessel is also shown. As can be seen from the figure the curve for the thin walled vessel (i.e., where a_{cr} approaches or exceeds t) is characterized by a significant reduction in failing stress at a given flaw size as compared to that for the thick walled vessel (i.e., where a_{cr} is small with respect to t).

2.2 INITIAL FLAW SIZES

While considerable emphasis is being placed upon development and application of nondestructive inspection procedures, the fact remains that defects can and do go undetected. The problem becomes increasingly acute with increases in material strength and the usually attendant reduction in toughness. Because of this, it is felt that the proof test is the most powerful inspection test presently available[1,2]. The knowledge gained in a successful proof test can be used to determine the maximum flaw size which can possibly exist in the vessel. Also, it can be seen that, having proof tested to a pressure of α times the maximum operating stress, the maximum possible applied stress intensity (K_{Ii}) which can exist at the time of applying the subsequent service cycle is $\frac{1}{\alpha} \times K_{Ic}$. This is of considerable significance because variations in actual material toughness (e.g., between weldments and base metal) and applied stress (e.g., at points of design discontinuities) do not affect this relationship. Application of this knowledge is discussed in Section 6.0 of this report.

2.3 SUBCRITICAL FLAW GROWTH

Probably the most predominant types of subcritical flaw growth are fatigue growth resulting from cyclic stress and environmentally induced sustained-stress growth. Also, growth may occur even in the absence of severe environmental effects if the initial flaw size approaches the critical flaw size[1].

The technique used for predicting the subcritical cyclic or sustained-stress flaw growth makes use of fracture specimen testing and the stress intensity concept. It has been shown[3,4,8] that the time or cycles to failure at a given maximum applied gross stress level depends primarily on the magnitude of the initial stress intensity at the flaw tip, K_{Ii}, compared to the critical stress intensity, K_{Ic} (i.e., cycles or time to failure = f (K_{Ii}/K_{Ic}). Thus, if cyclic or sustained-stress fracture specimens are used to obtain experimentally the K_{Ii}/K_{Ic} versus cycles or time curves for a material, the cycles or time required for any given initial flaw to grow to critical size can be predicted. Conversely, if the required life of the structure is known in terms of stress cycles or time at stress, the maximum allowable initial flaw size can be determined.

What normally is obtained from a plane strain fracture specimen cyclic or sustained test is the initial flaw size, the critical size as measured from the fracture face, the cycles or time it took to grow from initial to critical size and the applied cyclic sustained stress. From these data the initial stress intensity, K_{Ii}, and the critical stress intensity, K_{Ic}, can be calculated. Typical examples of K_{Ii}/K_{Ic} versus time curves are shown in Figure 4.

Of primary significance in sustained load tests is that there appears to be a threshold stress intensity level below which time dependent subcritical growth does not take place. While many pressure vessel material-environment combinations exhibit relatively high threshold values as shown in Figure 4, flaw growth at relatively low K levels has been observed (e.g., most high strength 4000 series steels in moist environments). Regardless, it is felt that to assure adequate life (for all vessels, with the possible exception of solid motor cases where operational requirements consist of only one short-time firing cycle) operation should be controlled at values below the observed threshold level. Below this level cyclic life is not significantly affected by total time at maximum stress. Above this level the cyclic growth rate is dependent upon cyclic speed.

3.0 MATERIALS

3.1 TITANIUM FORGINGS AND WELDMENTS

Base metal specimens tested in this program were machined from each of six 6Al-4V vessel forgings. Three of these were taken from Lunar Orbiter forgings originally supplied by Cameron Iron Works. These are essentially the same as some forgings used on Apollo reaction control system vessels. The remaining specimens were taken from Apollo SPS cylindrical tank forgings. All base metal specimens were machined from the forgings such that loading was parallel to the hoop direction.

Welded specimens were machined from girth welds taken from either of two Apollo SPS fuel tank assemblies welded by Allison Division of General Motors. These specimens were all machined such that loading was perpendicular to the weld centerline.

A summary of forging and weldments used in the tests is shown in Table I; available chemical compositions and heat treatments are shown in Table II.

3.2 TEST FLUIDS

As shown in Table I, a total of seven test fluids were investigated. The compositions of the fuels and oxidizer are shown in Tables III, IV, and V. Nitric oxide was added to available nitrogen tetroxide (MIL-P-26539B) to obtain the composition shown in Table III.

Methanol and Freon FM compositions are shown in Tables VI and VII. As noted, two different samples of Freon MF were used, both supplied by the Space and Information Systems Division of North American Avaiation (NAA). Both samples were reportedly taken from the same batch; the first was apparently badly contaminated during transfer and shipment. The distilled water was inhibited by adding 500 parts per million sodium-chromate.

4.0 EXPERIMENTAL PROCEDURES

4.1 SPECIMEN PREPARATION

Precracked surface flaw specimens were used for all static toughness, sustained load, and cyclic tests. Flaws were made by electric discharge machining a starter notch, and by extending the notch by low stress tension fatigue. The fatigue extension was accomplished at maximum gross stress levels of 30 to 40 KSI at 1800 cpm (from 5000 to 16,000 cycles were required, depending upon initial notch dimensions). For the majority of these tests, initial surface flaws were precracked in air before testing in the selected environment. Two additional series of tests were performed to check the influence of cracking history. This included precracking in methanol and Freon MF with subsequent testing in Aerozene 50 and N_2O_4, respectively. Base metal sustained load tests in methanol were also precracked in both air and methanol. Specimen blanks taken from the Lunar Orbiter forgings were solution treated and quenched, rough machined, aged in argon, finish machined, and then stress relieved in air (see Table II). Initial cracking was accomplished after heat treating. For all other specimens (i.e., the weldments and those taken from Apollo cylinders) the material was supplied in the fully heat treated and stress relieved condition, and were machined and precracked after receipt.

Overall dimensions for the surface flawed specimens were tailored to the size and shape of available material. Thickness of the Lunar Orbiter forgings was sufficient to allow the use of flat specimens, Figure 7b.

Welded specimens, shown in Figure 5 were machined flat in the gage area to provide a uniform section. Location of the surface flaw with respect to the weld structure is shown in Figure 6. This location was selected after cyclic testing of several specimens in methanol. Results indicated that crack initiation occurred most readily in the weld centerline followed closely by the location shown in Figure 6. The latter location was selected because applied stresses are higher at this point.

Dimensions of the base metal specimens are shown in Figure 7. The curvature noted in Figure 7a results from the original cylindrical contour. Flattening was not attempted because of potential breakage and because of unknown residual stresses. These curved specimens required the use of the stress intensity solution shown in Figure 7a which is based on the work of Smith[7]. The bending coefficient, M_B, is plotted in Figure 8. For the flaw shapes and sizes used it was found that the stress intensity was still maximum at the bottom of the flaw (i.e., at the angle $\psi = 0$). Bending stress was experimentally determined by mounting back-to-back strain gages on an unflawed specimen and loading slowly to failure. The resulting relation between uniform tension stress and bending stress is shown in Figure 9.

4.2 FLAW GROWTH TEST SETUP

The majority of sustained load test specimens were loaded in 10,000 lb dead-load creep machines. Those tests using nitrogen tetroxide, Aerozene 50, and monomethylhydrazene utilized a setup as shown in Figures 10, 11, and 12. Liquid was contained in two pressurized tanks connected with flex lines to each other and to a small cup clamped to the test specimen. Periodically, one of the tanks was raised or lowered so that the fluid would flow through the specimen cup thus supplying fresh liquid. Temperature was controlled by warm air supplied from Coates heaters. Schematic of the fluid and pressurization system is shown in Figure 13.

Nonhazardous sustained load tests were performed in an environmentally controlled laboratory at the Boeing Developmental Center. All but the 85°F/Freon MF tests were performed at atmospheric pressure with the test fluid and specimen contained in polyethylene bags. Fluid and specimens used in the 85°F/Freon MF tests were enclosed in a stainless steel jacket pressurized slightly above vapor pressure (i.e., 8 psig).

4.3 EXPERIMENTAL APPROACH FOR SUSTAINED LOAD TESTS

The approach used to define threshold stress intensity levels is shown schematically in Figure 14. The first surface flawed specimen (after determining the static K_{Ic} value) was loaded to a target stress intensity level less than critical (i.e., an initial stress intensity value, K_{Ii}). The specimen was held at constant load until failure or for a predetermined time (usually 24 to 48 hours). If failure did not occur, the specimen was cycled in air in low stress fatigue to mark the flaw front, and then was pulled to failure. Evidence of sustained load growth was then observed by a separation between the initial fatigue crack extension and that of the final marking. With either failure or evidence of growth in the first specimen, subsequent specimens were loaded at successively lower K_{Ii} values until neither failure nor growth took place. Usually, the threshold value was bracketed with three to four specimens.

5.0 TEST RESULTS

5.1 MECHANICAL PROPERTIES

Tensile and yield strength of the weldments and forgings that were tested in this program were measured at room temperature. The resulting properties are listed in Table VIII.

5.2 PLANE STRAIN FRACTURE TOUGHNESS

Plane strain toughness values (K_{Ic}) were determined at room temperature for a total of six different 6Al-4V forgings, and from the heat affected zone (HAZ) of two different weldments. A summary of the values obtained is shown in Table IX. As shown in the table, toughness values were obtained both by static tests as well as from sustained load test specimens which had not failed during the programmed sustained load period. In the case of weld sample #2, all values shown were taken from sustained load test specimens.

The average K_{Ic} values for the six forgings range from 41.5 to 48.6 KSI $\sqrt{IN}$, while the average HAZ values range from 39.3 to 40.8 KSI $\sqrt{IN}$ for the two weldments.

5.3 SUSTAINED LOAD FLAW GROWTH DATA

Sustained load subcritical flaw growth studies were performed with combinations of four forgings, two weld samples, seven liquid environments, and test temperatures ranging from 65 to 110°F. A summary of the test conditions is shown in Table I. Tabulation of the test data, showing precracking procedures, initial flaw sizes, test conditions and results is included in Tables X through XXII.

During initial tests of weld specimens (primarily those tested in Aerozene 50) attempt was made to control flaw shapes to an a/2c value of about 0.25. Actual shape ratios varied from 0.23 and higher. For these specimens initial stress intensities were calculated using Kobayashi's M_K solution for flaws of a/2c values of 0.29 and lower; Smith's M_K solution for flaws of a/2c values of 0.33 and greater; and an average M_K value between these extremes for intermediate shapes (see Figure 2). Use of these flaw shapes, while normally preferred, resulted in a requirement for loading at relatively high stresses for the high K_{Ii} levels. This in turn resulted in several weld centerline failures, outside of the flaw, possibly due to creep. This usually occurred when applied stress levels exceeded 110 KSI. In later tests, the flaw shape was revised to nominal a/2c values of 0.20, thus allowing reduction of applied stress at comparable K_{Ii} levels, and also allowing exclusive use of the Kobayashi deep flaw term.

As noted in Tables X through XXII, the initially applied stress intensity levels are shown in terms of a decimal fraction of K_{Ic}. In most cases, the average K_{Ic} value of previously tested specimens was used. For the first series of tests performed, (where only few samples were available for calculating average values) the K_{Ii} value was divided by the individual calculated end point K_{Ic} value. This latter method was also useful in cases where both initial and critical flaws either varied from the desired elliptical shape or were quite large with respect to the gross section area. In this case, the relative stress intensity ratio can be more accurately determined than can the absolute values. While the difference between the two methods is normally negligible, use of average rather than end point values is generally preferred for sustained load testing. This preference is based upon the fact that such growth can often result in irregular final flaw shapes, even though the initial flaw was relatively well shaped.

Results of the data shown in Tables X through XXII are plotted in Figures 15 through 27. Figure 28 shows the fracture appearance of the series of base metal specimen tests in monomethylhydrazene. The trend of increased slow growth with increased applied stress intensity is evidenced by the separation of the initial and the final cyclic crack extension. Other examples of fracture appearance are shown in Figures 29 through 32. All photos were taken using polarized white light techniques[4].

5.4 CYCLIC LOAD FLAW GROWTH DATA

Cyclic load subcritical flaw growth experiments were performed with combinations of two forgings, one weld sample, four liquid environments, and test temperatures ranging from 65 to 105°F. A summary of the test conditions is shown in Table I. All specimens in this series of tests were precracked in air. Cycling was performed at 5 CPM, with R = 0.05. Tabulation of the test data, showing precracking procedures, initial flaw sizes, test conditions, and results is included in Table XXIII.

6.0. DISCUSSION OF RESULTS

6.1 CRITICAL FLAW SIZES AND PREDICTED FAILURE MODE

The results of the plane strain fracture toughness tests are summarized in Table IX. It is seen that the overall average K_{Ic} values for the forgings and weld HAZ are 45.2 and 40.3 KSI $\sqrt{IN}$, respectively. Individual values varied about plus or minus ten percent of these averages, with variations within a given forging or weldment generally less than this spread.

Figure 33 relates critical flaw sizes with operating stress for the SPS fuel tank gages. The K_{Ic} values used represent averages taken from Allison supplied forging and weldment Sample #1. Flaw size is plotted in terms of depth, a, assuming small a/2c values (i.e., Q ≈ 1.0 and Kobayashi's M_K applies). The effect of deep flaw magnification is graphically evidenced by the two different forging curves, representing differences in vessel thickness.

Depending on thickness, it is seen that critical flaw depth at proof stress of 140 KSI varies from about 0.017 to 0.023 inches in the forged material. For a girth weld HAZ, assuming meridional proof stress of 57 KSI across the weld, calculated critical flaw depth is about 0.056 inches, or approximately 84 percent of the 0.067 inch thickness. For the above cases, failure during proof test would be expected to be catastrophic in nature, since critical flaw depths are less than the thickness.

Assuming maximum operating stresses of 75 percent of proof stress, it is seen that critical base metal flaw depths (for flaws oriented normal to maximum stress) are still less than the thickness. For the welds, the critical depth at maximum operating stress is now greater than the thickness, and leakage would be expected prior to complete failure.

6.2 ALLOWABLE FLAW SIZE CURVES - SUSTAINED LOAD

Table XXIV summarizes the threshold stress intensity ratios (i.e., K_{Ii}/K_{Ic} values) defined by the curves of Figures 15 through 27. Several general observations can be made from a review of the summary table, and the curves. In Figure 34, the effect of test temperature on threshold ratios are plotted for nitrogen tetroxide, Aerozene 50, and monomethylhydrazene. Included in the nitrogen tetroxide curve is the previously established threshold value for 0.25 percent NO content N_2O_4[9]. It is seen that increasing temperature is accompanied by a slight but measurable reduction in threshold level.

It is seen that threshold values are similar for base metal and weld HAZ in all environments tested except for Freon MF in which the HAZ threshold is significantly lower than the base metal value. Additionally, little difference is observed between the two series of Freon MF tests (i.e., 65°F tests using Freon sample #1, versus 85°F tests using Freon sample #2). It is possible that any effects which might have been caused by the increased temperature were compensated for by differences in the sample compositions.

Also, by observation of the data plotted in Figures 22, 23, 26, and 27, it appears that threshold values are not affected by the prior history of pre-cracking in either Freon MF or in methanol as compared to those specimens precracked in air. As seen in Figure 15, there is an effect of precracking environment on the rate of growth in the methanol tests.

Usefulness of the threshold values can best be realized by constructing composite critical and threshold flaw size curves. This is illustrated for the SPS fuel tank thicknesses and environments in Figures 35 through 37. The curves shown are based upon critical stress intensity values equal to the average values for the Allison supplied weldment #2 and cylindrical forging, "D". Threshold curves are based upon the percentage of these critical values as noted in Table XXIV. Again, flaw length is assumed large with respect to depth. Use of these curves is described in the following paragraphs based upon discussion of the data in Figure 35. The figure is based upon forging properties for the SPS fuel tank cylinder (0.053 inch wall thickness).

As shown in Figure 35, stress-flaw size curves are plotted representing critical values as well as threshold values in the environments of methonal, Aerozene 50 at two operating temperatures, monomethylhydrazene, and distilled and inhibited distilled water. Horizontal lines are scribed at stress levels representing proof pressure, maximum operating pressure, and nominal operating pressure. For vessels successfully passing the proof test, it is seen that the maximum initial flaw size existing at the time of the next test or operational cycle is 0.023 inches. Now consider the effect of subsequent pressurization in different environments at a maximum operating stress of 105 KSI. For example, initial flaws as small as 0.003 inches could have grown if exposed to methanol. This is significantly smaller than that guaranteed by the proof test. Depending upon the time involved in methanol tests, and the actual initial size, flaws greater than 0.003 inches could have grown to critical size (about 0.032 inches) and caused catastrophic failure. In cases where the vessel might have been successfully exposed to methanol (that is, where no failure occurred) at 105 KSI, it can be stated only that the flaw size after exposure did not exceed 0.032 inches. As a result, any additional vessel life at 105 KSI applied stress, regardless of the liquid environment, could not be guaranteed. Additional guarantees of successful performance, say in Aerozene 50, could be based either upon results of an additional proof test, or, as noted in Figure 35, if re-proof testing was not accomplished, by subsequent control of temperature and pressure equivalent to about 85 KSI at 70°F. This combination of temperature and stress results in a stress intensity less than the threshold value in Aerozene 50 for a vessel containing a 0.032 inch flaw.

For vessels which are to be exposed only to Aerozene 50 after the proof test, Figure 35 can also be used to depict allowable operating conditions. For example, it can be seen that at 105 KSI, flaw sizes of 0.023 (that size proved by the proof test) are marginally acceptable at operating temperatures exceeding 110°F.

Interpretation and application of the results shown in Figures 36 and 37 would be similar to that of the preceding discussion.

6.3 CYCLIC BEHAVIOR

Ideally, cyclic flaw growth data is best generated and utilized by the testing of relatively large specimens sized such that both initial as well as critical flaw size is small with respect to the specimen width and thickness. End point data curves from tests can then be directly differentiated to develop growth rate data (i.e., K_I versus da/dn curves). Application can then be made by integrating the developed curves and accounting for deep flaw magnification as applicable to the vessel gages in question (see Reference 10).

Another method of generating growth rate data involves measurement of incremental (or average) growth of several cyclic specimens. While this procedure allows some reduction of specimen size (critical stress intensity levels need not be attained), abnormally high applied stress levels are required at the higher applied K levels.

Unfortunately, the base metal and weldment material supplied, being representative in thickness to the actual pressure vessels, was too thin for such quantitative treatment. With virtually all specimens shown in Table XXIII, the flaw grew through-the-thickness at an unknown number of cycles prior to failure. Consequently, these results cannot be used to predict cyclic damage in tanks.

Some perspective can be gained by studying the results of the base metal cyclic tests performed in Aerozene 50 (see Table XXIII). In this case specimen thickness (0.125) was marginally adequate, and, while some deep flaw growth was encountered, failure occurred prior to the time the flaw grew through-the-thickness. This data was reduced to provide the rate curve shown in Figure 38. Using this curve, and referring to Figure 35, it can be roughly calculated that it would take approximately 170 full amplitude operating pressure cycles to grow a flaw (in the absence of a severe environment) from an 0.023 inch depth to an 0.026 inch depth. In other words, a vessel successfully passing proof test (K_{Ii}/K_{Ic} = 0.75 max) could be cycled about 170 times at 105 KSI before the stress intensity ratio would exceed the threshold in Aerozene 50 at 70°F (K_{Ii}/K_{Ic} = 0.82).

7.0 CONCLUSIONS

1. The sustained load flaw growth data for 6Al-4V titanium forgings in methanol shows that, at the operating stress levels in the Apollo SPS fuel tanks, initial flaws or defects of undetectable size can grow to critical size and cause failure.

2. If the flaws are oriented normal to the circumferential stress in the tank cylinder they can attain critical size prior to growing through the thickness and catastrophic fracture will result. This is apparent from the predicted critical flaw size curve (Figure 35) and is consistent with the second fuel tank failure at North American Aviation.

3. If the flaws are oriented normal to the meridional stress (e.g., in the weldments or weld HAZ) they will likely grow through the thickness prior to reaching critical size and leakage, rather than complete fracture, will result. This is apparent from the predicted critical flaw size curve (Figure 37) and is consistent with the first fuel tank failure at North American Aviation.

4. Although threshold values in Freon MF are substantially higher than in methanol, it cannot be guaranteed that potentially serious crack growth would not take place during Freon exposure.

5. With the exception of nitrogen tetroxide (above 85°F), methanol, and Freon MF, the sustained load threshold stress intensities for all other test fluids and propellants investigated were found to be 0.75 K_{Ic} or higher. For threshold values at 0.75 K_{Ic}, a successful proof test to at least 1/0.75 or 1.33 x maximum operating pressure should be sufficient to assure that the vessels do not contain flaws which will grow to critical size and cause failure at sustained operating pressures.

6. In that sustained stress flaw growth can occur in distilled water and inhibited distilled water if the initial stress intensity (flaw size and/or stress level) is large, it is concluded that time at proof pressure should be minimized.

7. From the standpoint of subcritical flaw growth, uninhibited distilled water appears to be superior to that which contains sodium chromate. This does not include possible differences in general (pitting) corrosion characteristics of the two liquids.

8. The environment does not have any major detrimental effect on cyclic flaw growth at stress intensity levels below the threshold value.

REFERENCES

1. ASTM Special Committee on Fracture Testing of High-Strength Metallic Materials, "Progress in the Measurement of Fracture Toughness and the Application of Fracture Mechanics to Engineering Problems", Materials Research and Standards, Vol. 4, No. 3, March 1964, p. 107.

2. ASTM STP 381, Fracture Toughness Testing and Its Applications, June 1964.

3. Tiffany, C. F., and P. M. Lorenz, "An Investigation of Low Cycle Fatigue Failures Using Applied Fracture Mechanics", May 1964, AF 33(657)-10251.

4. Tiffany, C. F., P. M. Lorenz, and R. L. Hall, "Investigation of Plane Strain Flaw Growth in Thick Walled Tanks", NASA CR-54837, February 1966.

5. Irwin, G. R., "Crack Extension Force for a Part-Through Crack in a Plate", Journal of Applied Mechanics, Vol. 84E, No. 4, December 1962.

6. Kobayashi, A. S., Boeing Structural Development Research Memorandum SDRM 16.

7. Smith, F. W., Boeing Structural Development Research Memorandum SDRM 17.

8. Tiffany, C. F., and F. A. Pall, "An Approach to the Pressure Vessel Minimum Fatigue Life Based upon Applied Fracture Mechanics", Boeing Document D2-22437, March 1963.

9. Haese, W. P., "Investigation of Fracture of 6Al-4V Titanium in N_2O_4", Boeing Document D2-24057-1, December 1965.

10. Tiffany, C. F., J. N. Masters, and F. A. Pall, "Some Fracture Considerations in the Design and Analysis of Spacecraft Pressure Vessels", presented at the ASM National Metals Congress, Chicago, October, 1966.

Table I : SUMMARY OF MATERIALS USED AND TESTS PERFORMED*

		METHANOL	DISTILLED H_2O	INHIBITED DISTILLED H_2O	FREON MF	MMH	AEROZENE 50	N_2O_4	STATIC TESTS
Lunar Orbiter Forging	A	S					S		✓
	B	S					S, C		✓
	C			S			S		✓
Apollo Cyl. (Allison S/N 73WCZ)	D		S, C	C	S, C	S		S	✓
Apollo Fuel Cylinders	#1								✓
	#2								✓
Weld Sample	#1	S	S	S	S		S, C		✓
	#2					S		S	**

* C = Cyclic Test
S = Sustained Load Test
✓ = Static K_{1c} Test

** K_{1c} Values Obtained From Sustained Load Test Specimens

Table II : MATERIAL COMPOSITIONS
(% By Weight)

	LUNAR ORBITER FORGINGS			APOLLO FORGINGS*	
	A	B	C	CYLINDER S/N 73WCZ "D"	DOME S/N 121WZU
ALUMINUM	6.2	6.25	6.10	6.3	6.45
VANADIUM	4.05	4.00	3.90	4.28	4.05
IRON	0.10	0.10	0.10	0.14	0.35
CARBON	0.036	0.062	0.040	0.020	0.03
HYDROGEN	0.0076	0.0075	0.0068	0.0084	0.0115
OXYGEN	0.190	0.193	0.191	0.190	0.170
NITROGEN	0.0085	0.0071	0.0090	0.0080	0.018
HEAT TREATMENT	Solution Treat 1750 °F-1 Hr, WQ Age 1050 °F-6 Hours In Argon, Air Cool Stress Relieve 1000 °F-4 Hours, Air Cool			Solution Treat & W Q Age 1100 °F-4 Hours Stress Relieve 1000 °F-4 Hours	

* Allison Analysis ; Cylinder S/N 73WCZ Is Designated As Forging "D" In This Report. Dome And CylindersNoted Are Also Used In Assy Of Weld Sample #1. Data On Weld Sample #2, And Apollo Fuel Cylinders #1 & #2 Are Not Available.

Table III : N_2O_4 COMPOSITION
(% By Weight)

PROPERTY	SAMPLE	SPECIFICATION LIMIT *
Nitric Oxide	0.49	0.6 ± 0.2
Water Equivalent	0.034	0.10 Max
Chloride As Nitrosyl Chloride	0.021	0.08 Max

* MSC-PPD-2A N_2O_4-INHIBITED

Table IV : AEROZENE 50 COMPOSITION
(% By Weight)

PROPERTY	SAMPLE	SPECIFICATION LIMIT*
N_2H_4 + UDMH	51.1 %	51.0 ± 0.8 %
N_2H_4	47.5 %	47.0 % Min
Water & Impurities	1.4 %	1.8 % Max

* MIL-P-27402

Table V : MONOMETHYLHYDRAZENE* COMPOSITION

PROPERTY	SAMPLE
MMH	99.8 %
Water	0.13 %
Transmittancy	98.0 %
Density Grams/Millimeter At 25 °C	0.871
Particulate Mg/Liter	0.20

* MIL-P-27404

Table VI : METHANOL COMPOSITION (% By Weight)

PROPERTY	LABEL ANALYSIS
Water	0.06 (0.04 Check)
Residue	0.0004
Acetone, Aldehydes	0.0003
Acidity (as HCOOH)	0.002
Alkalinity (as NH_3)	None
Cu & Ni	0.00001

Table VII : FREON MF COMPOSITION

PROPERTY	NAA SPEC. MB 0210-014 REQUIREMENT	UNUSED SAMPLE #1 FROM NAA	UNUSED SAMPLE #2 FROM NAA
Purity	99.8 % By Weight	>99.9 %	99.9 %
Acid	0.0001 % HCL Max	0.000097 %	0.0006 %
Moisture	10 ppm Max	2.6 ppm	14.8 ppm
Chloride Ion	0.1 ppm Max	0.13 ppm	0.04 ppm
Residue	2 ppm Max.	240* ppm	20 ppm

* Insufficient Sample Available To Run Determination Per Spec.

Table VIII : TENSILE DATA

MATERIAL		AVERAGE ULTIMATE STRENGTH, KSI	AVERAGE YIELD STRENGTH, KSI 0.2 % OFFSET	NUMBER OF SPECIMENS
Lunar Orbiter	Forging A	165.8	156.9	2
	Forging B	169.1	157.1	3
	Forging C	168.3	159.4	3
*Apollo Cyl. (Allison S/N 73WCZ)	Forging D	175.1	164.3	3
*Apollo Dome (Allison S/N 121WZU)	—	177.5	167.8	3
Weldment Sample	#1	132.7	126.4	2

* Allison Data

Table ~~IX~~ I : PLANE STRAIN FRACTURE TOUGHNESS VALUES

MATERIAL		APPROX. SPECIMEN THICKNESS (In)	AVERAGE STATIC K_{Ic} Ksi$\sqrt{In.}$	AVERAGE SUSTAINED K_{Ic} Ksi$\sqrt{In.}$	OVERALL AVERAGE K_{Ic} Ksi$\sqrt{In.}$	RANGE Δ RANGE	NUMBER OF MEASUREMENTS	STD. DEV. σ	K_{Ic} 99% PROB.
Lunar Orbiter	Forging A	0.125	43.3	44.2	43.6	42.9–44.2 1.3	3	.77	
	Forging B	0.125	43.5	46.08	45.3	38.8–48.1 9.3	7	3.44	
	Forging C	0.125	44.1	45.7	45.6	42.9–48.7 5.8	10	1.92	
	Forging C	0.02	43.5	—	43.5	39.2–47.7 8.5	2	7.56	
Apollo Cyl. (Allison S/N 73WCZ)	Forging D	0.058	45.2	46.0	45.8	44.8–46.4 1.6	5	.69	44.2
Apollo Fuel Cylinders	#1	0.057	48.6	-	48.6	48.2–49.0 0.8	2	1.78	
	#2	0.057	41.5	-	41.5	39.9–43.0 3.1	2	2.76	
Weldment Samples (H.A.Z.)	#1	0.045	39.1	39.4	39.3	36.9–44.2 7.3	5	3.14	32.0
	#2	0.045	-	40.8	40.8	38.2–43.0 4.8	9	1.63	

Table X: SUSTAINED LOAD FLAW GROWTH IN METHANOL
(Base Metal & H.A.Z. At R.T.)

MATERIAL			GROSS AREA	CRACK EXTENSION				SUSTAINED LOAD TEST				K_{Ii} KSI $\sqrt{IN.}$	TIME (HRS)	K_{Ic} KSI $\sqrt{IN}$		K_{Ii} / K_{Ic}	GROWTH
WELD	FORGING	SPECIMEN NUMBER		ENVIRON. A=Air M=Methanol F=Freon MF	MAX GROSS STRESS (KSI)	a_i (IN.)	$2C_i$ (IN.)	ENVIRONMENT	TEMPERATURE (°F)	AVG. PRESSURE (PSIG)	LOAD (LBS.)			AVERAGE	END POINT		
-	A	3	.0631	A	40.0	0.044	0.150	Methanol	72	0	7020	37.0	0.2 (1)	43.6	-	.848	YES(1)
-	A	13	.0628	A	40.0	0.057	0.155	"	72	0	6280	34.4	0.4 (1)	43.6	-	.789	YES(1)
-	A	12	.0630	M	40.0	0.061	0.164	"	72	0	5520	31.2	0.2 (1)	43.6	-	.716	YES(1)
-	A	14	.0629	A	40.0	0.046	0.142	"	72	0	5320	27.6	2.2 (2)	43.6	-	.633	YES
-	B	19	.0633	M	40.0	0.041	0.142	"	72	0	3460	17.0	4.9 (1)	45.3	-	.375	YES(1)
-	B	20	.0626	M	40.0	0.040	0.140	"	72	0	4450	22.4	2.8 (1)	45.3	-	.494	YES(1)
-	B	27	.0631	M	40.0	0.030	0.134	"	72	0	2260	10.2	47.5	45.3	-	.225	NO
I	-	W-11	.0223	M	40.0	0.024	0.088	"	72	0	2240	30.0	0.6 (1)	39.3	-	.763	YES(1)
I	-	W-12	.0249	M	40.0	0.026	0.096	"	72	0	1980	24.1	4.4 (1)	39.3	-	.613	YES(1)
I	-	W-16	.0228	M	40.0	0.027	0.097	"	72	0	1195	16.5	6.5 (1)	39.3	-	.420	YES(1)
I	-	W-17	.0246	M	40.0	0.026	0.096	"	72	0	890	10.9	190.4	39.3	-	.277	NO

NOTES:
(1) Failure
(2) Failed outside of flawed area; specimen was welded together, marked, and pulled to failure (see Figure 33)

Table XI : SUSTAINED LOAD FLAW GROWTH IN DISTILLED WATER
(Base Metal & Weld H. A. Z. At 65 °F)

MATERIAL			GROSS AREA	CRACK EXTENSION				SUSTAINED LOAD TEST				K_{Ii} KSI $\sqrt{IN.}$	TIME (HRS)	K_{Ic} KSI$\sqrt{IN.}$		K_{Ii} / K_{Ic}	GROWTH
WELD	FORGING	SPECIMEN NUMBER		ENVIRON. A=Air M=Methanol F=Freon MF	MAX GROSS STRESS (KSI)	a_i (IN.)	$2C_i$ (IN.)	ENVIRONMENT	TEMPERATURE (°F)	AVG. PRESSURE (PSIG)	LOAD (LBS.)			AVERAGE	END POINT		
-	D	D-1	0.0283	A	30.0	0.030	0.128	Water	65	0	3280	41.9	50.8	-	46.9	.893	YES
-	D	D-10	0.0284	A	30.0	0.024	0.127	"	65	0	3200	37.3	58.2	-	44.4	.840	NO
-	D	D-21	0.0288	A	30.0	0.024	0.131	"	65	0	3078	35.2	24.7	-	46.1	.764	NO
-	D	D-22	0.0291	A	30.0	0.027	0.121	"	65	0	2948	33.7	45.3	45.8	-	.736	NO
I	-	W-31	0.0219	A	40.0	0.025	0.116	"	65	0	2112	31.6	59.9	39.3	-	.804	NO
I	-	W-29	0.0214	A	40.0	0.031	0.120	"	65	0	1930	35.4	48.9	39.3	-	.901	YES

Table XII : SUSTAINED LOAD FLAW GROWTH IN INHIBITED DISTILLED WATER[1]
(Base Metal & Weld H.A.Z. At R.T.)

MATERIAL			GROSS AREA	CRACK EXTENSION				SUSTAINED LOAD TEST				K_{I1} KSI $\sqrt{IN.}$	TIME (HRS)	K_{Ic} KSI$\sqrt{IN}$		K_{I1} / K_{Ic}	GROWTH
WELD	FORGING	SPECIMEN NUMBER		ENVIRON. A=Air M=Methanol F=Freon MF	MAX GROSS STRESS (KSI)	a_1 (IN.)	$2C_1$ (IN.)	ENVIRONMENT	TEMPERATURE (°F)	AVG. PRESSURE (PSIG)	LOAD (LBS.)			AVERAGE	END POINT		
-	C	38	.0606	A	40.0	0.038	0.127	Inhib. H_2O (1)	72	0	7320	37.7	117.5	-	43.5	.867	YES
-	C	39	.0639	A	40.0	0.034	0.128	"	72	0	8020	38.4	144.7	-	47.1	.814	NO
-	C	40	.0629	A	40.0	0.046	0.144	"	72	0	7800	41.3	147.2	-	48.7	.848	YES
-	C	41	.0626	A	40.0	0.039	0.133	"	72	0	8020	41.0	< 0.1 (2)	45.6	-	.899	YES (2)
-	C	42	.0637	A	40.0	0.040	0.135	"	72	0	8020	41.2	< 0.1 (2)	45.6	-	.904	YES (2)
-	C	43	.0629	A	40.0	0.040	0.134	"	72	0	7880	40.0	153.5	-	48.0	.833	YES
-	C	44	.0623	A	40.0	0.044	0.137	"	72	0	7940	41.5	153.3	45.6	-	.910	YES
-	C	45	.0627	A	40.0	-	-	"	72	0	(3)	-	-	-	-	-	-
I	-	W-26	.0221	A	40.0	0.032	0.124	"	65	0	2130	38.3	51.7	39.3	-	.974	YES
I	-	W-27	.0221	A	40.0	0.025	0.111	"	65	0	2040	30.3	52.4	39.3	-	.771	TRACE
I	-	W-34	.0216	A	40.0	0.026	0.127	"	65	0	1893	30.3	24.7	39.3	-	.771	NO

NOTES:
(1) 500 PPM Sodium Chromate
(2) Failure
(3) Failed on loading

Table XIII : SUSTAINED LOAD FLAW GROWTH IN FREON MF (1)
(Base Metal & Weld H. A. Z. At 65 °F)

MATERIAL			GROSS AREA	CRACK EXTENSION				SUSTAINED LOAD TEST				K_{I1} KSI $\sqrt{IN.}$	TIME (HRS)	K_{Ic} KSI$\sqrt{IN}$		K_{I1} / K_{Ic}	GROWTH
WELD	FORGING	SPECIMEN NUMBER		ENVIRON. A=Air M=Methanol F=Freon MF	MAX GROSS STRESS (KSI)	a_1 (IN.)	$2C_1$ (IN.)	ENVIRONMENT	TEMPERATURE (°F)	AVG. PRESSURE (PSIG)	LOAD (LBS.)			AVERAGE	END POINT		
-	D	D-5	.0287	A	30.0	0.029	0.129	Freon MF(1)	65	0	3330	40.9	(20 secs.)(2)	45.8	-	.893	YES(2)
-	D	D-8	.0283	A	30.0	0.026	0.129	"	65	0	3093	37.4	0.15 (2)	45.8	-	.816	YES(2)
-	D	D-9	.0283	A	30.0	0.026	0.121	"	65	0	3005	35.4	47.4	-	46.4	.763	TRACE
-	D	D-11	.0285	A	30.0	0.029	0.132	"	65	0	3200	40.4	(30 secs)(2)	45.8	-	.882	YES (2)
-	D	D-15	.0282	A	30.0	0.026	0.125	"	65	0	2820	33.7	48.4	45.8	-	.736	YES
-	D	D-17	.0288	A	30.0	0.028	0.133	"	65	0	2969	36.8	0.1(2)	45.8	-	.807	YES (2)
-	D	D-20	.0286	A	30.0	0.027	0.123	"	65	0	2718	32.9	0.2(2)	45.8	-	.718	YES (2)
-	D	D-23	.0292	A	30.0	0.027	0.126	"	65	0	2630	31.0	0.6(2)	45.8	-	.677	YES (2)
-	D	D-24	.0292	A	30.0	0.025	0.127	"	65	0	2480	28.1	0.6(2)	45.8	-	.614	YES (2)
-	D	D-25	.0287	A	30.0	0.026	0.122	"	65	0	2295	27.0	26.0	-	46.3	.583	NO
I	-	W-28	.0238	A	40.0	0.028	0.115	"	65	0	1890	26.8	0.2(2)	39.3	-	.682	YES (2)
I	-	W-30	.0218	A	40.0	0.028	0.120	"	65	0	1965	32.0	0.05(2)	39.3	-	.814	YES (2)
I	-	W-32	.0217	A	40.0	0.027	0.125	"	65	0	1380	22.2	48.2	39.3	-	.565	YES
I	-	W-33	.0220	A	40.0	0.025	0.119	"	65	0	1562	23.3	0.2(2)	39.3	-	.593	YES (2)
I	-	W-35	.0218	A	40.0	0.031	0.127	"	65	0	1310	23.6	0.2(2)	39.3	-	.601	YES (2)
I	-	W-36	.0202	A	40.0	0.026	0.120	"	65	0	1112	19.2	28.3	39.3	-	.488	YES
I	-	W-37	.0219	A	40.0	0.029	0.130	"	65	0	898	15.1	44.4	39.3	-	.384	NO

NOTES:
(1) Freon MF from sample #1 (see Table VII)
(2) Failure

Table XIV: SUSTAINED LOAD FLAW GROWTH IN FREON MF (1)
(Base Metal & Weld H.A.Z. At 85 °F)

MATERIAL			GROSS AREA	CRACK EXTENSION				SUSTAINED LOAD TEST				K_{Ic} KSI√IN.				
WELD	FORGING	SPECIMEN NUMBER		ENVIRON. A=Air M=Methanol F=Freon MF	MAX GROSS STRESS (KSI)	a_i (IN.)	$2C_i$ (IN.)	ENVIRONMENT	TEMPERATURE (°F)	AVG. PRESSURE (PSIG)	LOAD (LBS.)	K_{Ii} KSI √IN.	TIME (HRS)	AVERAGE	END POINT	K_{Ii} / K_{Ic}	GROWTH
-	D	D-52	.0292	A	30	0.026	0.136	Freon MF (1)	85	8	2440	29.0	24.0	45.8	-	.633	No
-	D	D-53	.0274	A	30	0.028	0.134	"	85	8	2460	31.9	23.0	45.8	-	.696	TRACE
-	D	D-54	.0288	A	30	0.027	0.122	"	85	8	2690	34.2	23.0	45.8	-	.747	YES
-	D	D-55	.0285	A	30	0.028	0.130	"	85	8	2420	29.9	24.0	45.8	-	.653	YES
-	D	D-57	.0288	A	30	0.028	0.128	"	85	8	3070	36.9	0.15 (2)	45.8	-	.806	YES (2)
I	-	W-66	.0220	A	30	0.028	0.128	"	85	8	1157	18.9	0.4 (2)	39.3	-	.481	YES (2)
I	-	W-67	.0214	A	30	0.029	0.122	"	85	8	942	16.2	24.0	39.3	-	.412	NO
I	-	W-68	.0211	A	30	0.024	0.115	"	85	8	1456	22.3	0.3 (2)	39.3	-	.567	YES (2)

NOTES:
(1) Freon MF from sample #2 (see Table VII)
(2) Failure

Table XV : SUSTAINED LOAD FLAW GROWTH IN MONOMETHYLHYDRAZENE
(Base Metal & Weld H. A. Z. At 105 °F)

MATERIAL			GROSS AREA	CRACK EXTENSION				SUSTAINED LOAD TEST				K_{I1} KSI $\sqrt{IN.}$	TIME (HRS)	K_{Ic} KSI$\sqrt{IN}$		K_{I1} / K_{Ic}	GROWTH
WELD	FORGING	SPECIMEN NUMBER		ENVIRON. A=Air M=Methanol F=Freon MF	MAX GROSS STRESS (KSI)	a_1 (IN.)	$2C_1$ (IN.)	ENVIRONMENT	TEMPERATURE (°F)	AVG. PRESSURE (PSIG)	LOAD (LBS.)			AVERAGE	END POINT		
-	D	D-47	.0290	A	30.0	0.029	0.119	MMH	106	175	2730	29.9	24.0	45.8	-	.653	NO
-	D	D-48	.0289	A	30.0	0.027	0.126	"	106	175	3120	36.9	24.0	45.8	-	.806	YES
-	D	D-49	.0324	A	30.0	0.031	0.142	"	108	175	3940	44.4	24.4	45.8	-	.969	YES
-	D	D-50	.0281	A	30.0	0.030	0.129	"	104	175	3230	41.8	23.9	45.8	-	.913	YES
-	D	D-51	.0290	A	30.0	0.025	0.127	"	107	175	2930	33.5	24.2	45.8	-	.731	NO
II	-	AW-39	.0238	A	30.0	0.023	0.113	"	102	175	2140	27.2	24.0	-	40.4	.673	NO
II	-	AW-41	.0217	A	30.0	0.024	0.112	"	107	175	2170	31.9	24.0	-	41.7	.764	TRACE
II	-	AW-42	.0232	A	30.0	0.024	0.117	"	103	175	1860	25.0	26.7	-	40.8	.613	NO
II	-	AW-43	.0193	A	30.0	0.025	0.120	"	105	175	1800	32.6	24.1	40.8	-	.799	YES
II	-	AW-44	.0215	A	30.0	0.026	0.127	"	103	175	2360	39.1	3.2 (1)	40.8	-	.958	YES (1)
II	-	AW-45	.0222	A	30.0	0.025	0.114	"	105	175	2530	-	(2)	-	-	-	-

NOTES:
(1) **Failure**
(2) **Failed on loading**

Table XVI : SUSTAINED LOAD FLAW GROWTH IN AEROZENE 50
(Base Metal At 65 - 79 °F)

MATERIAL			GROSS AREA	CRACK EXTENSION				SUSTAINED LOAD TEST				K_{I1} KSI $\sqrt{IN.}$	TIME (HRS)	K_{Ic} KSI$\sqrt{IN}$		K_{I1} / K_{Ic}	GROWTH
WELD	FORGING	SPECIMEN NUMBER		ENVIRON. A=Air M=Methanol F=Freon MF	MAX GROSS STRESS (KSI)	a_i (IN.)	$2C_i$ (IN.)	ENVIRONMENT	TEMPERATURE (°F)	AVG. PRESSURE (PSIG)	LOAD (LBS.)			AVERAGE	END POINT		
-	A	5	.0630	M	40.0	0.044	0.146	Aerozene	79	0	7400	38.9	18.5	-	44.2	.880	YES
-	A	6	.0622	M	40.0	0.063	0.170	"	-	-	(1)	-	-	-	-	-	-
-	A	8	.0630	M	40.0	-	-	"	-	-	(1)	-	-	-	-	-	-
-	A	9	.0623	M	40.0	0.059	0.173	"	-	-	(1)	-	-	-	-	-	-
-	A	10	.0630	M	40.0	0.068	0.190	"	74	0	5500(2)	33.3(3)	6.0	-	37.7	.883	YES
-	A	11	.0621	M	40.0	-	-	"	-	-	(1)	-	-	-	-	-	-
-	B	16	.0629	M	40.0	0.042	0.138	"	70	0	7100	36.7	27.2	45.3	-	.810	NO (4)
-	B	17	.0633	M	40.0	0.036	0.138	"	65	0	6700	33.0	40.5	-	46.7	.707	NO
-	B	18	.0626	M	40.0	0.038	0.136	"	68	0	7430	37.5	239.8	-	44.6	.841	TRACE
-	B	22	.0629	M	40.0	0.037	0.134	"	65	0	8400	42.4	< 0.1 (5)	45.3	-	.935	YES (5)
-	B	23	.0621	M	40.0	0.034	0.130	"	73	0	8100	40.4	26.4	-	48.1	.840	YES
-	B	24	.0627	M	40.0	0.038	0.141	"	70	0	8300	42.9	< 0.1 (5)	45.3	-	.947	YES (5)
-	B	25	.0634	M	40.0	0.042	0.141	"	73	0	(6)	38.3	144.0	-	46.0	.833	TRACE
-	B	28	.0632	A	40.0	0.027	0.133	"	70	0	8100	37.5	46.7	-	45.0	.833	NO

NOTES:

(1) Failed on loading
(2) ±50# cyclic load @ 5 CPS
(3) Initial & critical values are depressed because of low W/2c values.
(4) This specimen was then cycled to failure; see Table
(5) Failure
(6) Cycled between 5700 & 7450# @ 2 hours per cycle.

Table XVII : SUSTAINED LOAD FLAW GROWTH IN AEROZENE 50
(Base Metal At 110 °F)

MATERIAL			GROSS AREA	CRACK EXTENSION				SUSTAINED LOAD TEST				K_{I1} KSI $\sqrt{IN.}$	TIME (HRS)	K_{Ic} KSI$\sqrt{IN}$		K_{I1} / K_{Ic}	GROWTH
WELD	FORGING	SPECIMEN NUMBER		ENVIRON. A=Air M=Methanol F=Freon MF	MAX GROSS STRESS (KSI)	a_i (IN.)	$2C_i$ (IN.)	ENVIRONMENT	TEMPERATURE (°F)	AVG. PRESSURE (PSIG)	LOAD (LBS.)			AVERAGE	END POINT		
-	B	29	.0629	A	40.0	0.039	0.141	Aerozene	98	85	8100	(1)	62.5	-	(1)	-	YES
-	C	30	.0633	A	40.0	0.029	0.133	"	105	85	8200	38.9	6.2 (2)	45.6	-	.853	YES (2)
-	C	31	.0634	A	40.0	0.040	0.131	"	110	150	6600	32.6	26.8	-	42.9	.759	YES
-	C	32	.0633	A	40.0	0.031	0.124	"	112	150	6750	31.5	40.7	-	47.3	.666	NO
-	C	33	.0632	A	40.0	0.040	0.134	"	108	230	6750	33.8	40.3	-	44.2	.765	NO
-	C	34	.0619	A	40.0	0.041	0.128	"	110	230	6950	35.2	72.9	-	44.1	.798	TRACE
-	C	35	.0623	A	40.0	-	-	-	-	-	(3)	-	-	-	-	-	-
-	C	36	.0608	A	40.0	0.043	0.131	"	108	230	7450	39.0	49.7	-	45.6	.855	YES

NOTES:
(1) Irregular flaw shape
(2) Failure
(3) Failed on loading

Table XVIII : SUSTAINED LOAD FLAW GROWTH IN AEROZENE 50
(Weld H. A. Z.)

MATERIAL				CRACK EXTENSION				SUSTAINED LOAD TEST						K_{Ic} KSI$\sqrt{IN}$			
WELD	FORGING	SPECIMEN NUMBER	GROSS AREA	ENVIRON. A=Air M=Methanol F=Freon MF	MAX GROSS STRESS (KSI)	a_i (IN.)	$2C_i$ (IN.)	ENVIRONMENT	TEMPERATURE (°F)	AVG. PRESSURE (PSIG)	LOAD (LBS.)	K_{I1} KSI $\sqrt{IN.}$	TIME (HRS)	AVERAGE	END POINT	K_{I1} / K_{Ic}	GROWTH
I	-	W-3	.0235	M	50.0	0.025	0.082	Aerozene	110	150	2640	30.7	25.9	39.3	-	.781	TRACE
I	-	W-4	.0234	M	50.0	0.027	0.089	"	110	150	2570	31.6	83.0	-	36.9	.856	YES
I	-	W-5	.0235	M	50.0	0.021	0.078	"	110	150	2800	32.0	2.1 (1)	39.3	-	.814	YES
I	-	W-7	.0214	M	40.0	0.025	0.092	"	85	150	2300	33.4	23.4 (2)	39.3	-	.850	YES(2)
I	-	W-8	.0228	M	40.0	0.031	0.093	"	105	150	2600	31.6	46.8 (2)	39.3	-	.804	YES(2)
I	-	W-10	.0223	M	40.0	0.026	0.095	"	105	150	2300	33.3	32.6	-	39.6	.841	YES
I	-	W-15	.0229	M	40.0	-	-	"	110	150	2500(3)	(4)	-	-	-	(4)	
I	-	W-18	.0197	A	40.0	0.019	0.084	"	110	150	2000	27.8	156.1	39.3	-	.707	NO
I	-	W-19	.0208	A	40.0	0.025	0.088	"	110	150	2200	32.9	82.3 (1)	39.3	-	.837	YES
I	-	W-20	.0225	M	40.0	0.026	0.092	"	112	150	2500(3)	35.2	12.3 (1)	39.3	-	.896	YES
I	-	W-21	.0210	M	40.0	0.025	0.090	"	112	230	2125	32.1	23.3	-	36.9	.870	TRACE
I	-	W-23	.0205	M	40.0	0.023	0.100	"	108	230	2050	31.4	33.1	39.3	-	.799	TRACE
I	-	W-24	.0205	A	40.0	0.025	0.091	"	108	150	2300	35.5	1.1 (1)	39.3	-	.903	TRACE
I	-	W-25	.0203	A	40.0	0.041	0.104	"	104	230	2175	34.0	.6 (2)	39.3	-	.865	YES(2)

NOTES:
(1) Failure in weld ℄ during sustained load: flaw size determined by sectioning
(2) Failed
(3) ±50# cyclic load @ 10 CPS
(4) Overload failure, flaw obscured.

Table XIX : SUSTAINED LOAD FLAW GROWTH IN N_2O_4 [1]
(Base Metal & Weld H.A.Z. At 70 °F)

MATERIAL: WELD	MATERIAL: FORGING	MATERIAL: SPECIMEN NUMBER	GROSS AREA	CRACK EXTENSION: ENVIRON. A=Air M=Methanol F=Freon MF	CRACK EXTENSION: MAX GROSS STRESS (KSI)	CRACK EXTENSION: a_i (IN.)	CRACK EXTENSION: $2C_i$ (IN.)	SUSTAINED LOAD TEST: ENVIRONMENT	SUSTAINED LOAD TEST: TEMPERATURE (°F)	SUSTAINED LOAD TEST: AVG. PRESSURE (PSIG)	SUSTAINED LOAD TEST: LOAD (LBS.)	K_{Ii} KSI $\sqrt{IN.}$	TIME (HRS)	K_{Ic} KSI$\sqrt{IN}$: AVERAGE	K_{Ic} KSI$\sqrt{IN}$: END POINT	K_{Ii} / K_{Ic}	GROWTH
-	D	D-36	.0282	A	30.0	0.024	0.126	N_2O_4	73	175	3240	37.6	24.0	45.8	-	.821	NO
-	D	D-37	.0328	A	30.0	0.022	0.117	"	70	175	3440	32.3	24.0	45.8	-	.705	NO
-	D	D-43	.0290	A	30.0	0.027	0.131	"	71	175	3500	41.6	21.7	45.8	-	.908	YES
-	D	D-59	.0283	A	30.0	-	-	"	-	-	(2)	-	-	-	-	-	-
II	-	AW-59	.0227	A	30.0	0.026	0.121	"	73	175	2290	34.0	24.0	40.8	-	.833	TRACE
II	-	AW-60	.0203	A	30.0	0.025	0.123	"	71	175	2150	36.9	24.0	40.8	-	.904	YES
II	-	AW-61	.0211	A	30.0	0.023	0.111	"	71	175	1930	28.7	24.1	40.8	-	.703	NO
I	-	W-69	.0212	A	30.0	0.021	0.118	"	72	175	1980	27.9	24.0	39.3	-	.710	NO

NOTES:
(1) No content 0.49%
(2) Failed on loading

Table XX : SUSTAINED LOAD FLAW GROWTH IN N_2O_4[1]
(Base Metal & Weld H.A.Z. At 85 ^{0}F)

MATERIAL			GROSS AREA	CRACK EXTENSION				SUSTAINED LOAD TEST				K_{Ii} KSI $\sqrt{IN.}$	TIME (HRS)	K_{Ic} KSI$\sqrt{IN}$		K_{Ii} / K_{Ic}	GROWTH
WELD	FORGING	SPECIMEN NUMBER		ENVIRON. A=Air M=Methanol F=Freon MF	MAX GROSS STRESS (KSI)	a_i (IN.)	$2C_i$ (IN.)	ENVIRONMENT	TEMPERATURE (°F)	AVG. PRESSURE (PSIG)	LOAD (LBS.)			AVERAGE	END POINT		
-	D	D-26	.0292	A	30.0	0.039	0.128	N_2O_4	85	35	3285	39.2	24.9	45.8	-	.855	YES
-	D	D-27	.0281	A	30.0	0.030	0.131	"	85	35	3320	43.0	24.0	45.8	-	.939	YES
-	D	D-28	.0291	A	30.0	0.025	0.125	"	84	35	3550	39.8	24.0	45.8	-	.869	YES
-	D	D-29	.0289	A	30.0	0.030	0.131	"	85	35	2660	33.6	24.0	45.8	-	.734	NO
-	D	D-58	.0285	A	30.0	0.025	0.125	"	84	175	2995	35.2	22.0	45.8	-	.768	NO
II	-	AW-46	.0236	A	30.0	0.027	0.118	"	85	175	2620	37.7	0.1 (2)	40.8	-	.924	YES(2)
II	-	AW-47	.0224	A	30.0	0.025	0.122	"	84	175	2370	34.9	72.0	40.8	-	.855	YES
II	-	AW-48	.0189	A	30.0	0.025	0.121	"	86	175	1900	36.0	26.7 (3)	40.8	-	.882	YES(3)
II	-	AW-49	.0201	A	30.0	0.024	0.114	"	86	175	1930	31.8	24.0	40.8	-	.779	TRACE
II	-	AW-40	.0177	A	30.0	0.023	0.115	"	87	175	1580	29.1	24.1	-	42.9	.678	NO
II	-	AW-55	.0226	A	30.0	0.024	0.122	"	84	175	1810	25.6	24.0	-	39.7	.644	NO
II	-	AW-56	.0225	A	30.0	0.026	0.122	"	85	175	2500	38.3	0.1 (2)	40.8	-	.939	YES(2)
II	-	AW-58	.0227	A	30.0	0.022	0.121	"	85	175	2090	27.8	59.9	-	38.9	.715	NO

NOTES:
(1) No content 0.49%
(2) Failure
(3) Flaw grew through-the-thickness

Table XXI : SUSTAINED LOAD FLAW GROWTH IN N_2O_4(1)
(Base Metal At 105 °F)

MATERIAL			GROSS AREA	CRACK EXTENSION				SUSTAINED LOAD TEST				K_{I1} KSI $\sqrt{IN.}$	TIME (HRS)	K_{Ic} KSI$\sqrt{IN}$		K_{I1} / K_{Ic}	GROWTH
WELD	FORGING	SPECIMEN NUMBER		ENVIRON. A=Air M=Methanol F=Freon MF	MAX GROSS STRESS (KSI)	a_i (IN.)	$2c_i$ (IN.)	ENVIRONMENT	TEMPERATURE (°F)	AVG. PRESSURE (PSIG)	LOAD (LBS.)			AVERAGE	END POINT		
-	D	D-30	.0285	A	30.0	0.026	0.125	N_2O_4	102	35	3300	39.4	24.2	45.8	-	.860	YES
-	D	D-32	.0284	A	30.0	0.028	0.126	"	105	35	2800	34.4	24.1	45.8	-	.751	YES
-	D	D-33	.0289	A	30.0	0.026	0.127	"	108	35	3490	40.7	22.0	45.8	-	.888	YES
-	D	D-31	.0288	A	30.0	0.028	0.132	"	100	35	3110	38.3	24.2	45.8	-	.836	YES
-	D	D-35	.0292	A	30.0	0.028	0.128	"	104	35	3650	43.8	24.3	45.8	-	.956	YES
-	D	D-34	.0290	A	30.0	0.030	0.133	"	105	35	2490	31.3	43.7	45.8	-	.683	NO
-	D	FD-39	.0289	F	30.0	0.023	0.116	"	106	35	3350	36.1	24.1	45.8	-	.788	YES
-	D	FD-41	.0292	F	30.0	0.027	0.132	"	105	35	2380	28.4	32.5	45.8	-	.620	NO
-	D	FD-40	.0292	F	30.0	0.026	0.127	"	109	35	2690	31.1	51.3	45.8	-	.679	NO

NOTE:
(1) No content 0.49%

Table XXII : SUSTAINED LOAD FLAW GROWTH IN N_2O_4 (1)
(Weld H.A.Z. At 105 °F)

MATERIAL			GROSS AREA	CRACK EXTENSION				SUSTAINED LOAD TEST				K_{I1} KSI $\sqrt{IN.}$	TIME (HRS)	K_{Ic} KSI$\sqrt{IN}$		K_{I1} / K_{Ic}	GROWTH
WELD	FORGING	SPECIMEN NUMBER		ENVIRON. A=Air M=Methanol F=Freon MF	MAX GROSS STRESS (KSI)	a_1 (IN.)	$2C_1$ (IN.)	ENVIRONMENT	TEMPERATURE (°F)	AVG. PRESSURE (PSIG)	LOAD (LBS.)			AVERAGE	END POINT		
II	-	AW-62	.0221	A	30.0	0.026	0.111	N_2O_4	106	175	2230	33.9	23.3	40.8	-	.831	YES
II	-	AW-63	.0227	A	30.0	0.023	0.115	"	102	175	1930	26.3	24.2	-	41.2	.638	NO
II	-	AW-64	.0220	A	30.0	0.021	0.116	"	108	175	1960	25.9	23.0	-	38.2	.678	NO
II	-	AW-65	.0214	A	30.0	0.022	0.119	"	107	175	1990	28.7	23.0	40.8	-	.703	TRACE
II	-	AW-50	.0220	F	30.0	0.023	0.112	"	106	175	2330	33.1	24.0	40.8	-	.811	YES
II	-	AW-51	.0216	F	30.0	0.026	0.116	"	103	175	2180	34.6	24.1	40.8	-	.848	YES
II	-	AW-52	.0226	F	30.0	0.024	0.117	"	105	175	1920	27.0	23.9	40.8	-	.662	NO
II	-	AW-53	.0217	F	30.0	0.023	0.120	"	104	175	2000	29.1	21.1	40.8	-	.713	TRACE
II	-	AW-54	.0221	F	30.0	0.024	0.109	"	105	175	1750	24.6	22.1	40.8	-	.603	NO

Table XXIII : CYCLIC FLAW GROWTH IN VARIOUS ENVIRONMENTS

MATERIAL			GROSS AREA	CRACK EXTENSION				CYCLIC LOAD TEST				K_{Ii} KSI $\sqrt{IN.}$	CYCLES TO FAILURE	K_{Ic} KSI$\sqrt{IN.}$		K_{Ii} / K_{Ic}	GROWTH
WELD	FORGING	SPECIMEN NUMBER		ENVIRON. A=Air M=Methanol F=Freon MF	MAX GROSS STRESS (KSI)	a_i (IN.)	$2c_i$ (IN.)	ENVIRONMENT	TEMPERATURE (°F)	AVG. PRESSURE (PSIG)	LOAD (LBS.) (1)			AVERAGE	END POINT		
-	D	D-12	.0286	A	30.0	0.026	0.124	Freon MF	65	0	2860	33.6	171	45.8		.734	
-	D	D-14	.0281	A	30.0	0.027	0.128	"	65	0	2136	26.3	595	"		.574	
-	D	D-16	.0301	A	30.0	0.030	0.127	"	65	0	1505	19.1	4116	"		.417	
-	D	D-13	.0286	A	30.0	0.023	0.129	Inhib. H_2O(2)	75	0	2860	32.2	338	"		.703	
-	D	D-6	.0323	A	30.0	0.023	0.128	"	75	0	2422	24.5	1744	"		.535	
-	D	D-18	.0291	A	30.0	0.026	0.128	"	75	0	2182	25.9	1054	"		.566	
-	D	D-7	.0280	A	30.0	0.025	0.134	Water	75	0	2800	34.0	122	"		.742	
-	D	D-3	.0368	A	30.0	0.027	0.130	"	75	0	2760	25.6	757	"		.559	
-	D	D-19	.0288	A	30.0	0.024	0.128	"	75	0	2016	23.4	1369	"		.511	
-	B	16	.0629	M	40.0	0.043	0.140	Aerozene	72	0	5500	27.8	1755	45.3		.614	
-	B	21	.0636	M	40.0	0.035	0.142	"	72	0	8000	41.7	96	45.3		.921	
I	-	W-13	.0236	M	40.0	0.025	0.0944	"	110	150	2700	34.9	1044	39.3		.888	
I	-	W-14	.0233	M	40.0	0.026	0.0948	"	97	150	2700	36.2	516	39.3		.921	

NOTES:
(1) Max load, R = .05, 5 CPM
(2) 500 PPM Sodium Chromate

Table XXIV:
SUMMARY OF SUSTAINED LOAD THRESHOLD VALUES

ENVIRONMENT	TEMP °F	THRESHOLD - K_{Ii}/K_{Ic}	
		BASE METAL	WELD H.A.Z.
Methanol	72	.24	.28
Distilled H_2O	65	.86	.86
Inhibited Distilled H_2O	72	.82	.82
Freon M.F.	65 (1)	.58	.40
	85 (2)	.58+	.40
MMH	105	.75	.75
Aerozine 50	65-79	.82	—
	110	.75	.75
N_2O_4 (3)	70	.81	.81
	85	.77	.77
	105	.70	.69
	115 (4)	.65	—

(1) Freon Sample # 1 } See Table VII
(2) Freon Sample # 2 }
(3) No Content 0.49% Except As Noted
(4) Data From Ref 9, No Content 0.25%

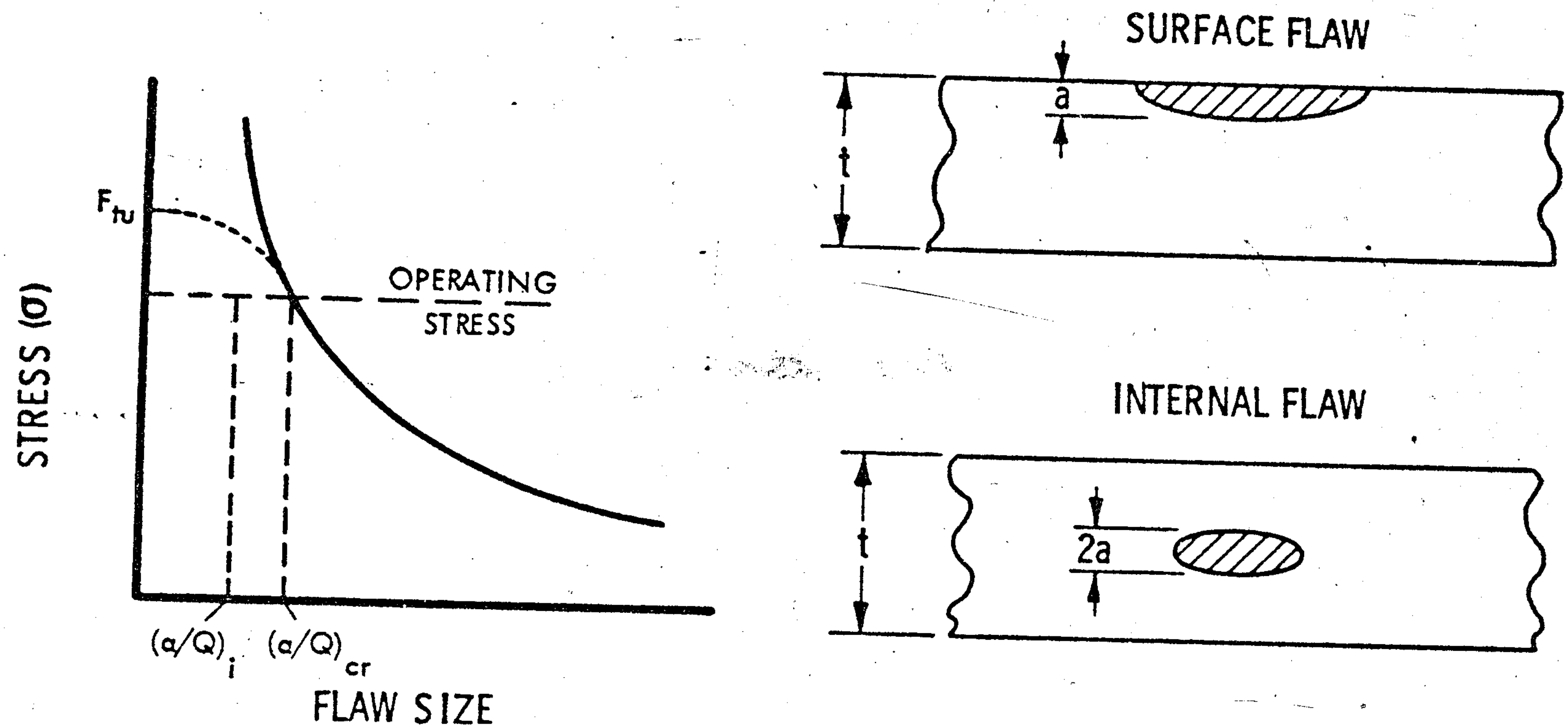

STRESS INTENSITY EQUATION:

$$K_{1c} = 1.1^{*} \sqrt{\pi}\ \sigma\ (a/Q)_{cr}^{1/2}$$

*Coef. Equal to Unity for Internal Flaws

WHERE:

σ = Applied Stress

Q = Shape Parameter (Ref. 1)

K_{1c} = Plane Strain Fracture Toughness

a = Flaw Depth (1/2 Depth for Internal Flaws)

FIGURE 1: APPLIED STRESS VS. CRITICAL FLAW SIZE

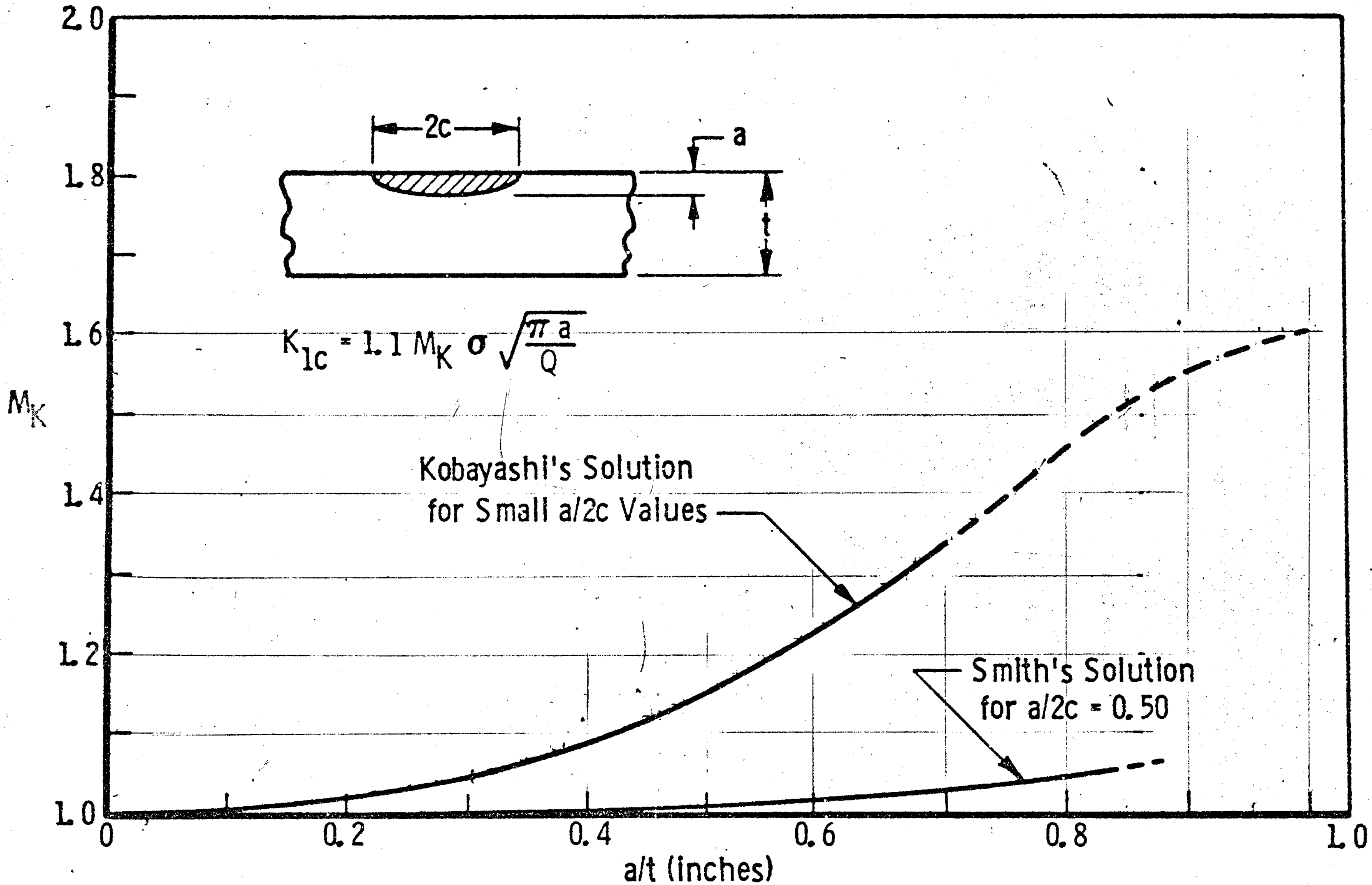

FIGURE 2: STRESS INTENSITY MAGNIFICATION FACTORS FOR DEEP SURFACE FLAWS

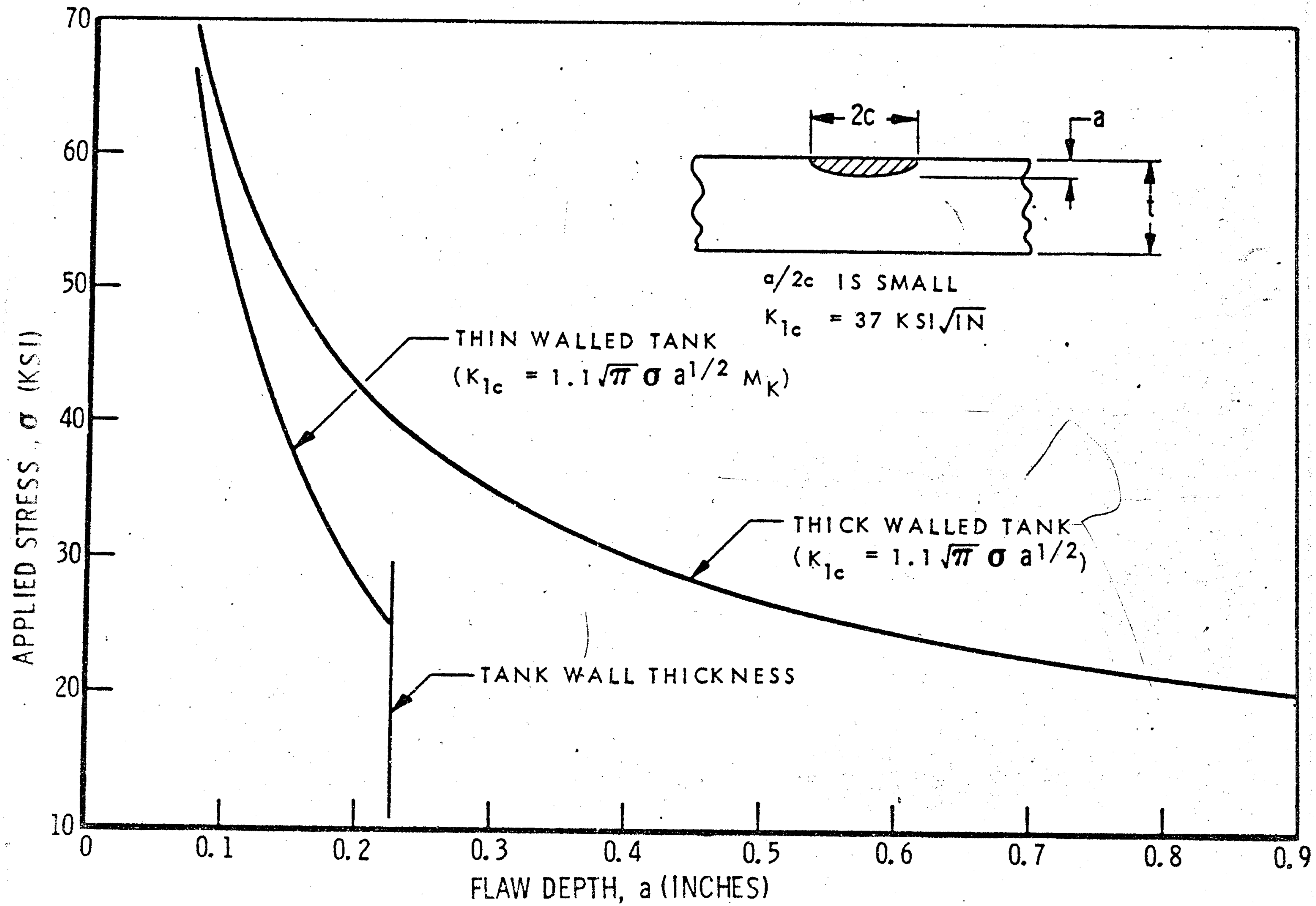

Figure 3 : CRITICAL FLAW SIZE CURVES (2219-T87 Aluminum At -320 °F)

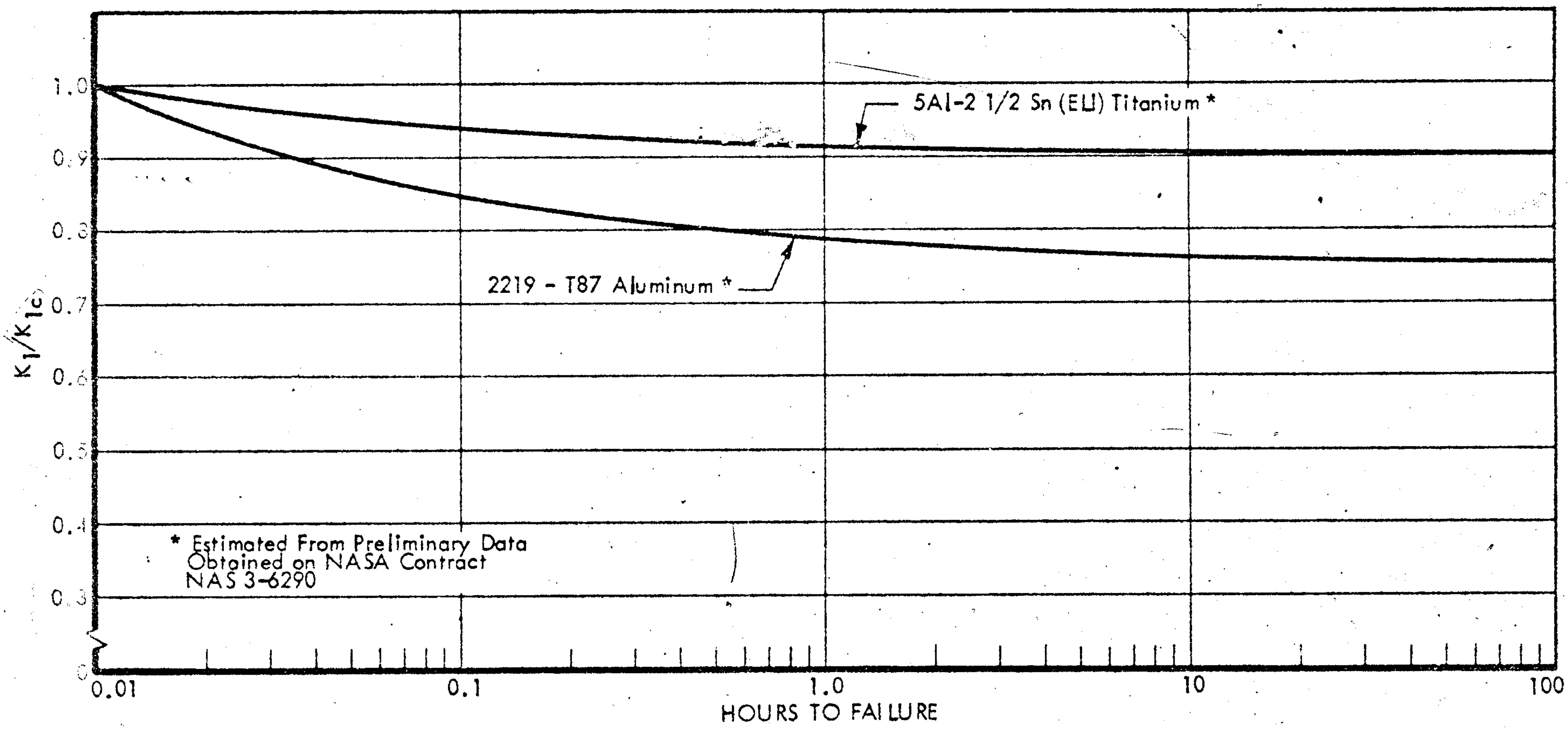

Figure 4 : SUSTAINED LOAD FLAW GROWTH CURVES FOR 2219-T87 ALUMINUM & 5AL-2 1/2 Sn (ELI) TITANIUM AT -320 °F & -423 °F

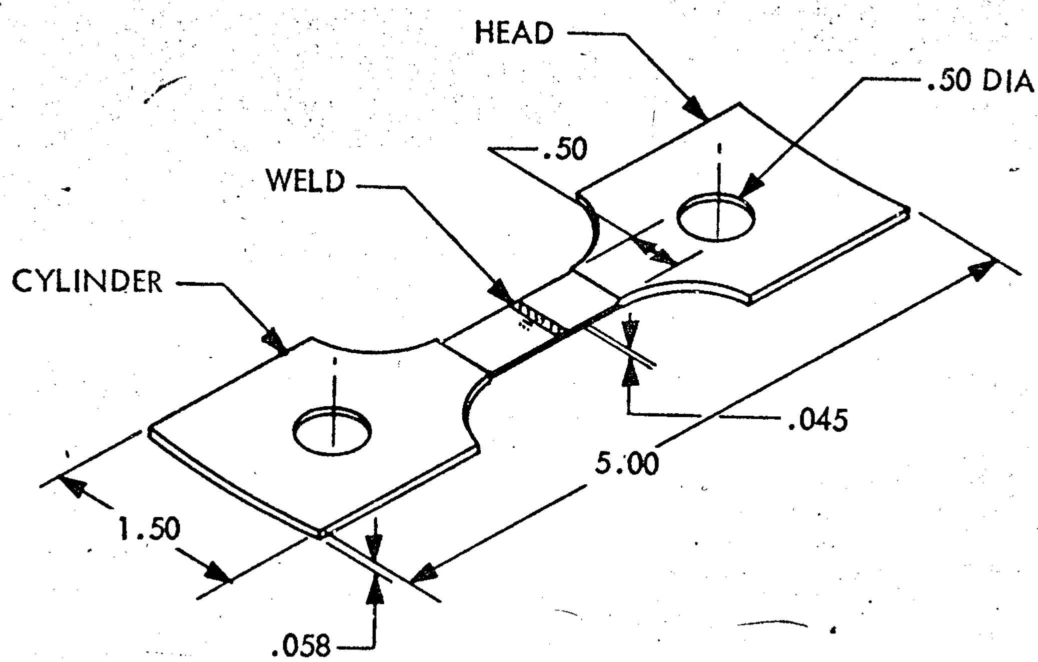

Figure 5: WELD SPECIMEN CONFIGURATION

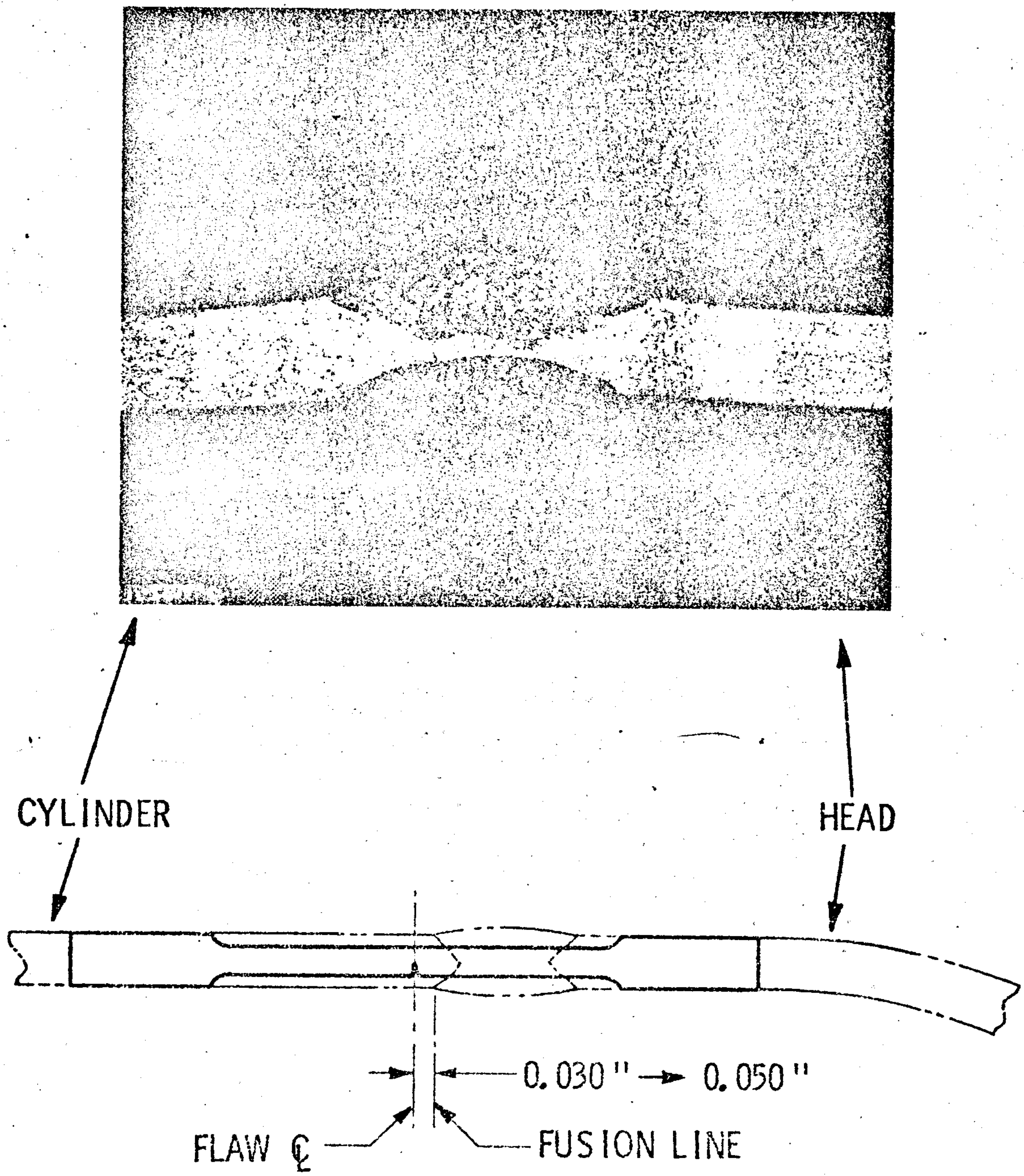

Figure 6 : FLAW PLACEMENT DETAIL (WELD SPECIMEN)

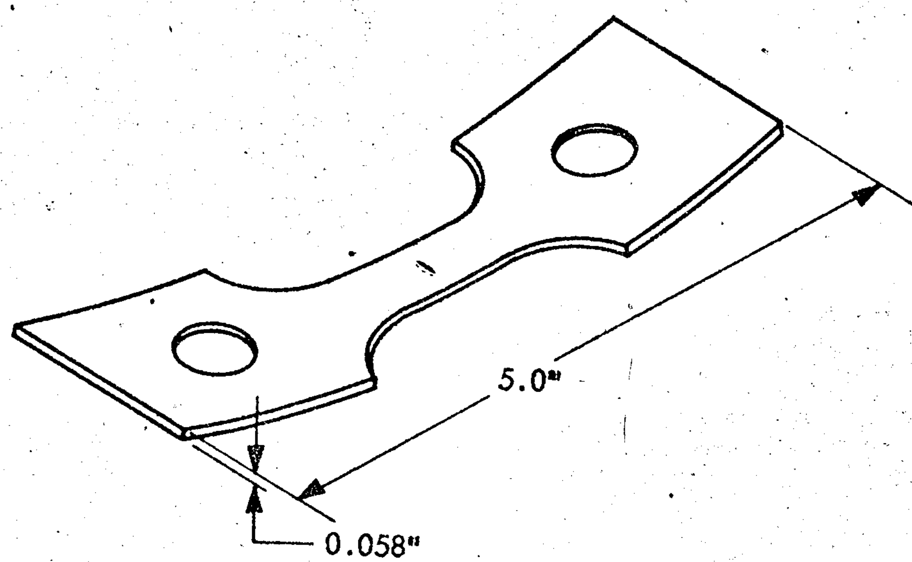

Figure 7a : ALLISON AND N.A.A. CYLINDERS

$$(K = 1.1\sqrt{\pi}\ \sigma_T\ (a/Q)^{1/2} M_K + M_B\sqrt{\pi}\ \sigma_B\ (a/Q)^{1/2}$$

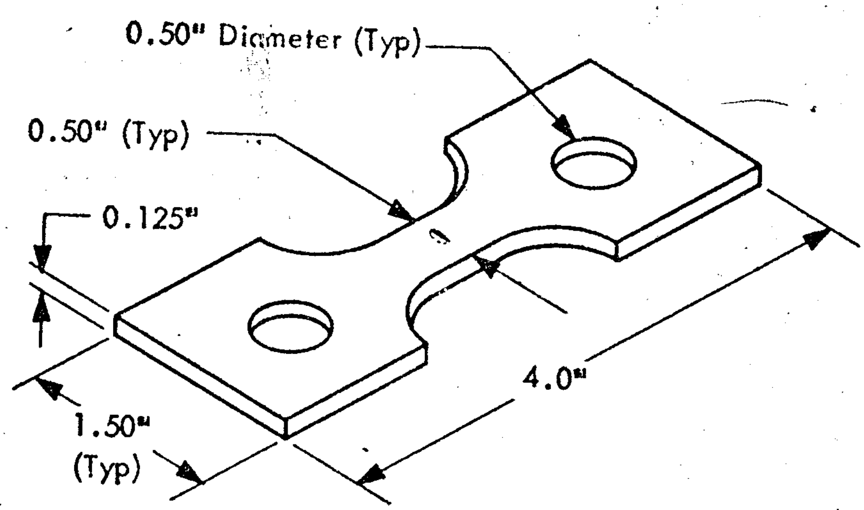

Figure 7b : LUNAR ORBITER FORGING STOCK

$$(K = 1.1\sqrt{\pi}\ \sigma_T\ (a/Q)^{1/2} M_K$$

Figure 7 : BASE METAL SPECIMEN CONFIGURATION

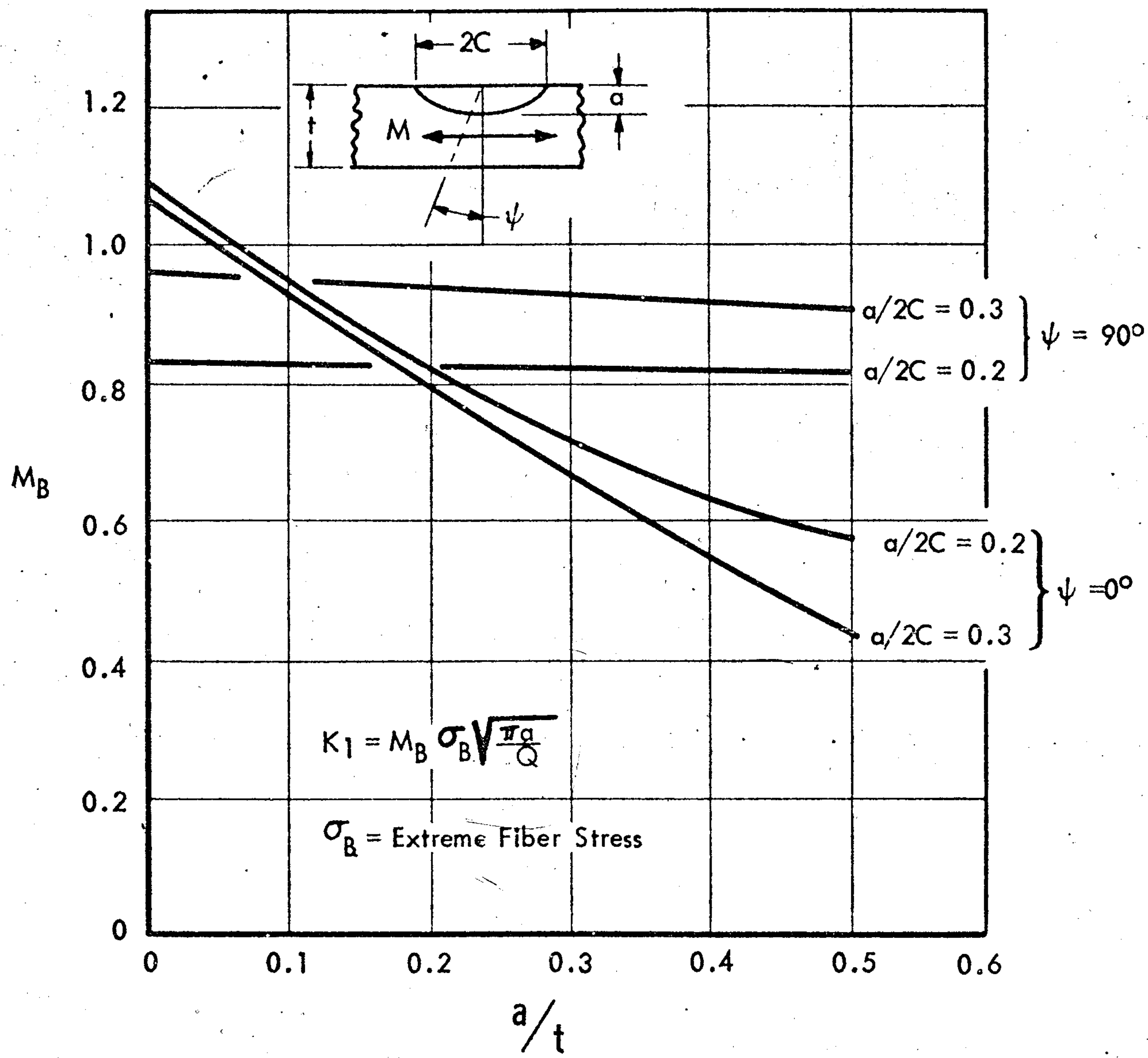

Figure 8 : APPROXIMATE STRESS INTENSITY FACTORS FOR SURFACE FLAWS IN BENDING

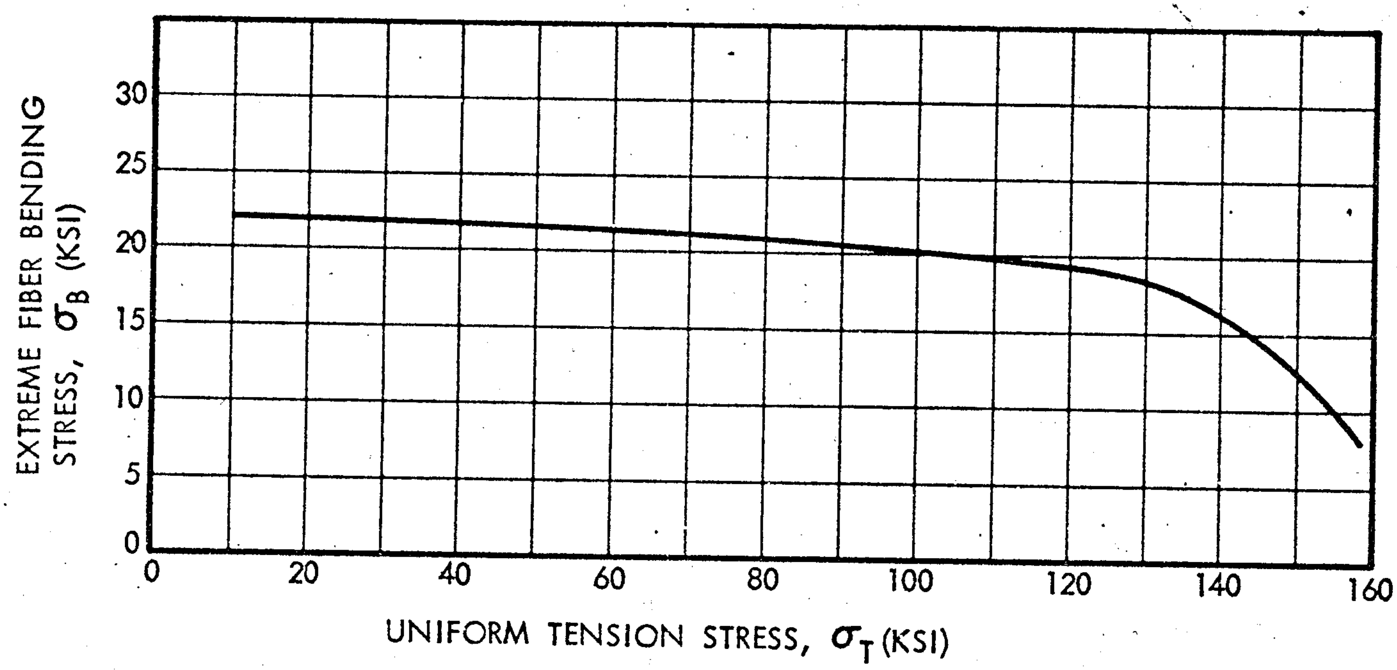

Figure 9 : BENDING STRESS IN CURVED SPECIMENS

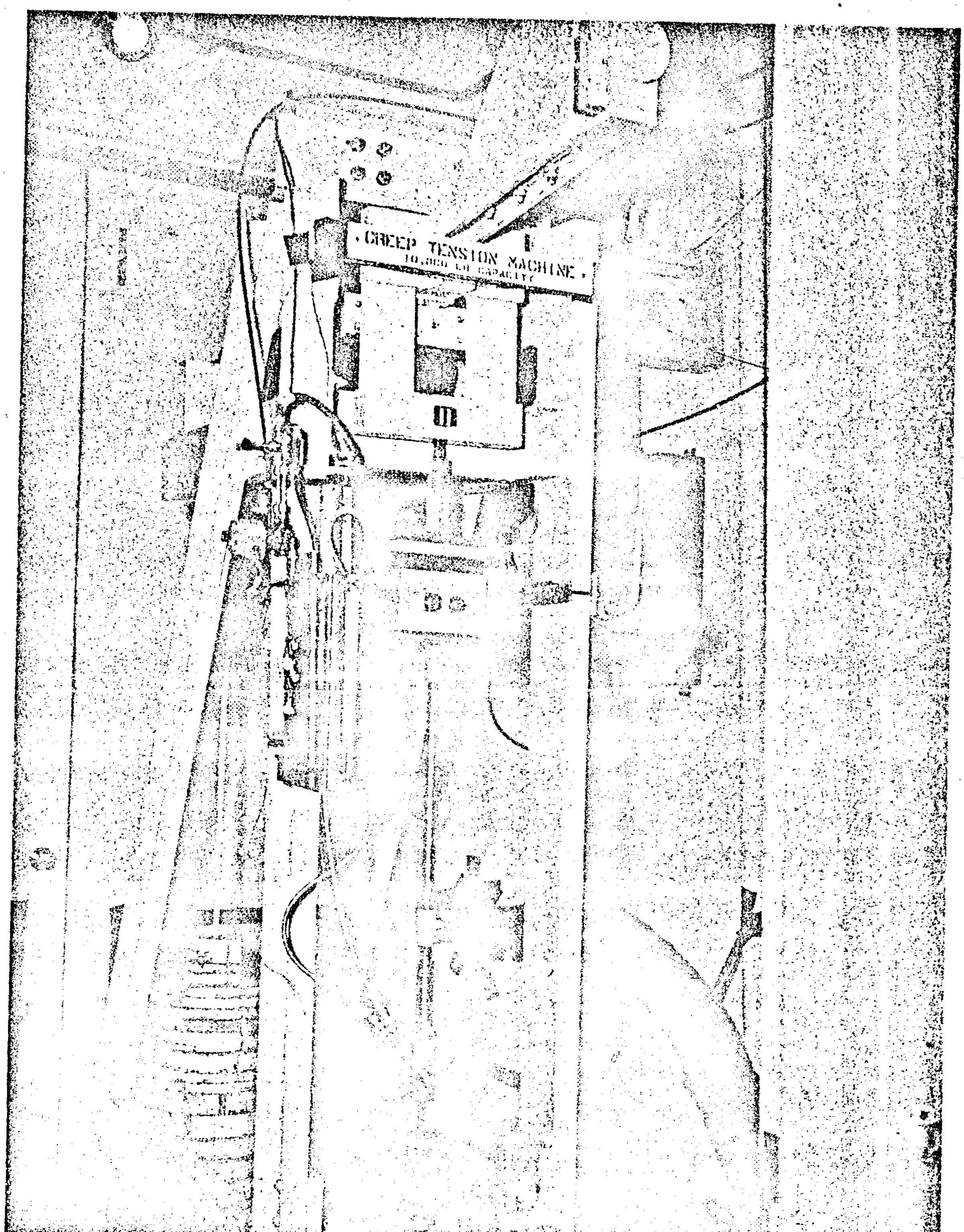

Figure 10 : AEROZENE SUSTAINED LOAD TEST SETUP - OVERALL VIEW

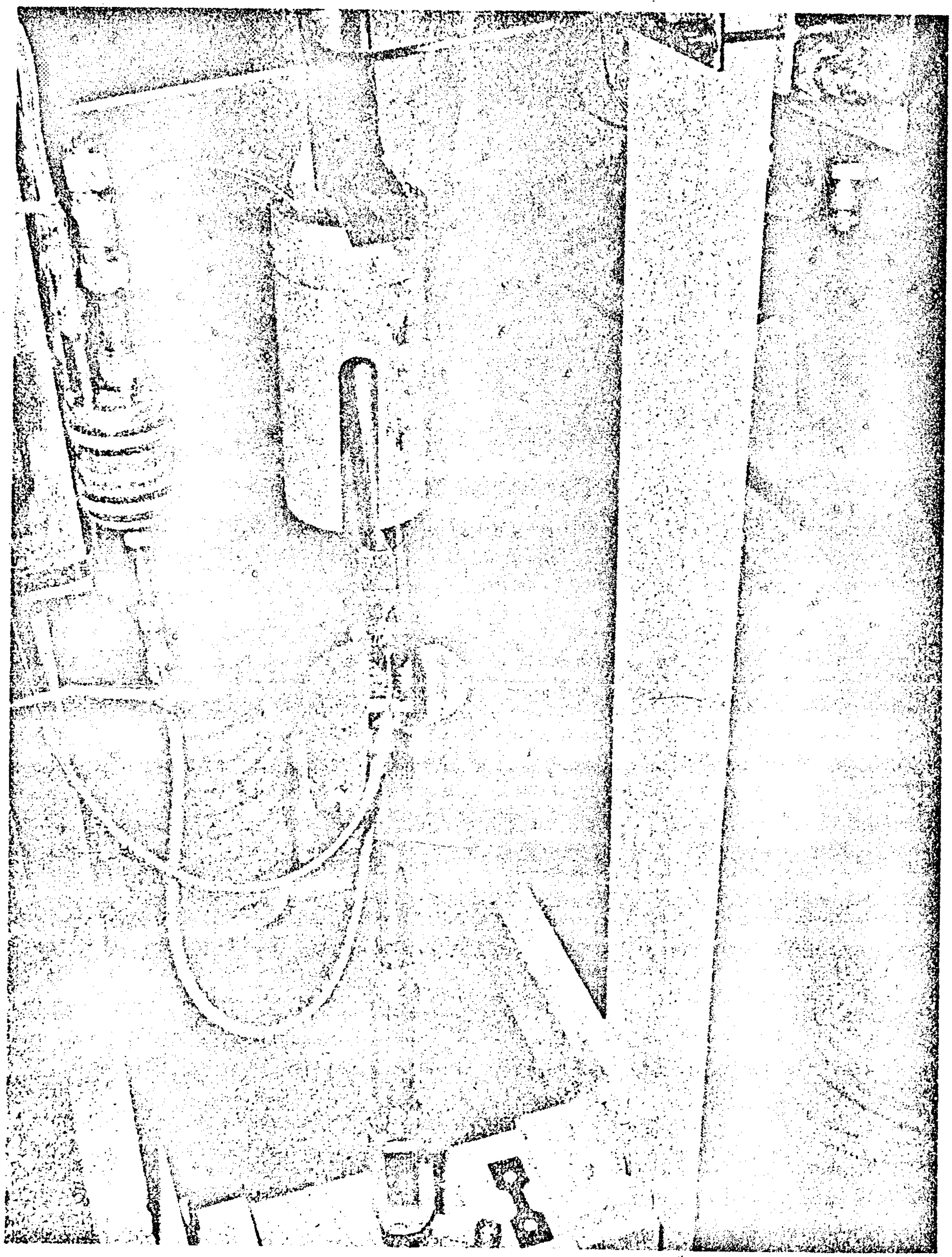

Figure 11 : AEROZENE SUSTAINED LOAD TEST SETUP - SHOWING SPECIMEN MOUNTING DETAIL

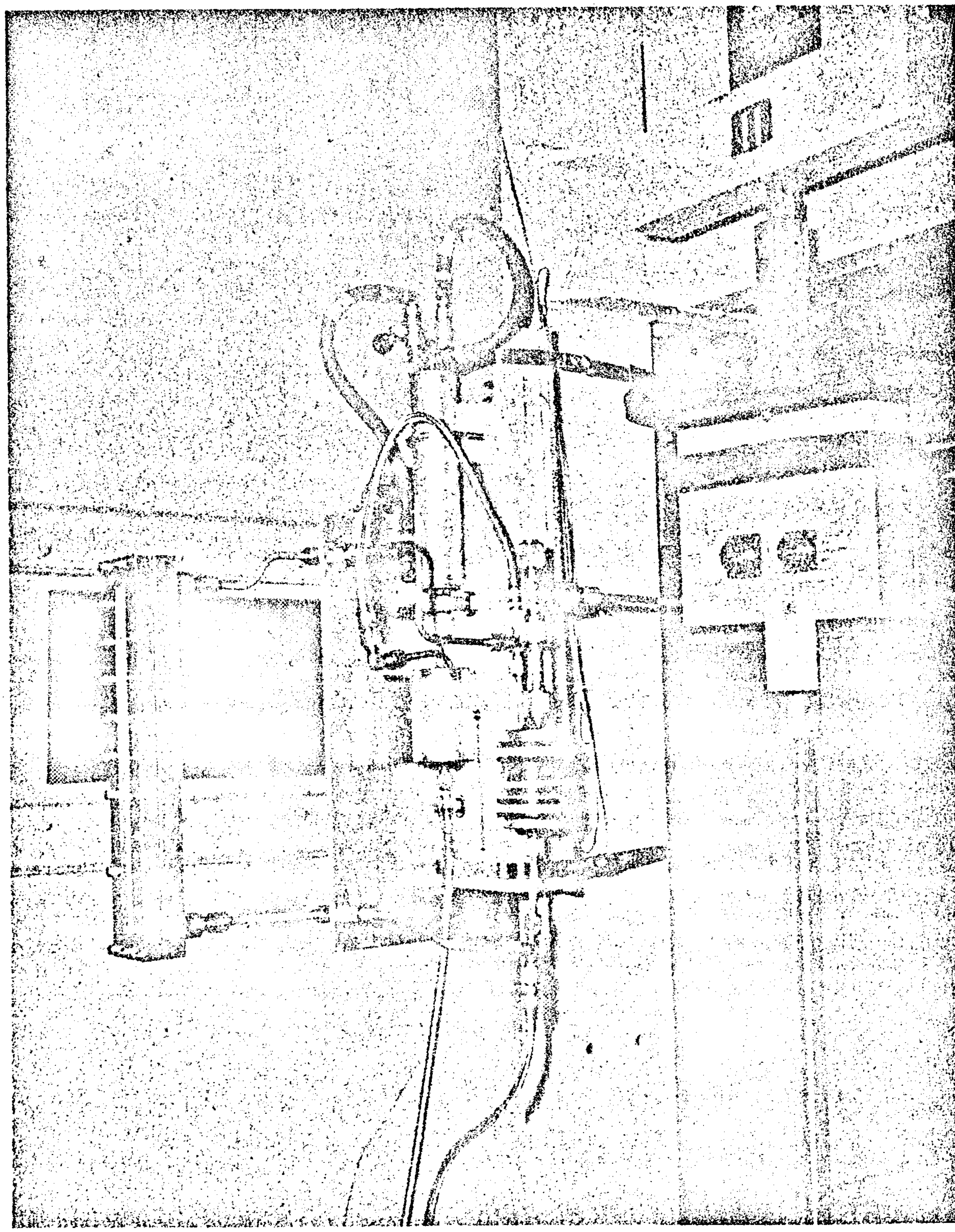

Figure 12 : AEROZENE SUSTAINED LOAD TEST SETUP - SHOWING AEROZENE SUPPLY SYSTEM

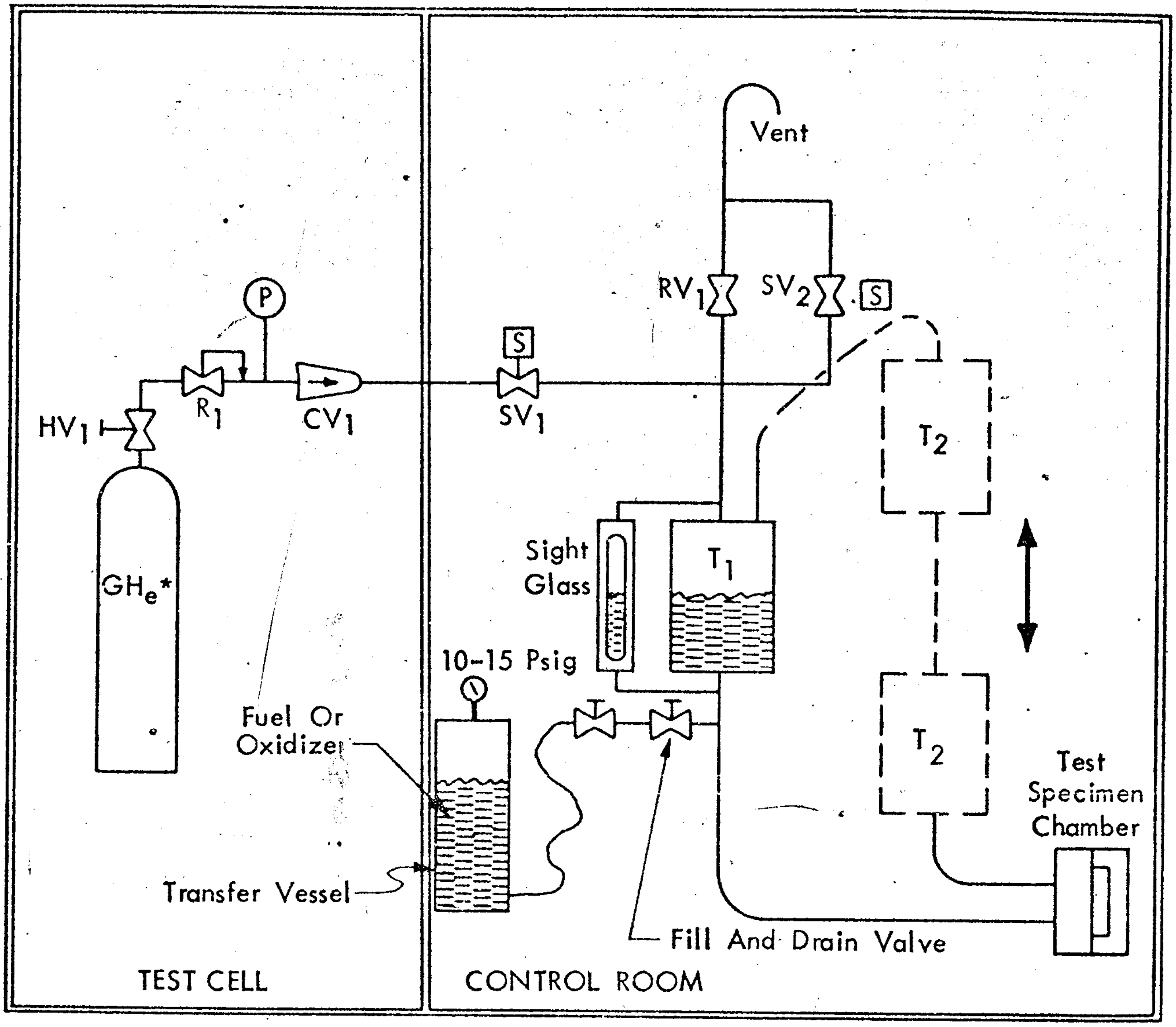

T_1 = Circulating Tank - Stationary

T_2 = Circulating Tank - Cycling

SV_1 = Normally Closed Solinoid Valve, 115 Vac

SV_2 = Normally Open Solinoid Valve, 115 Vac (Vent Valve)

RV_1 = Relief Valve, 280 Psig

CV_1 = Check Valve, 300 Psi

* H_e System Also Used For Purging System

Figure 13 : FLUID AND PRESSURIZATION SYSTEM SCHEMATIC

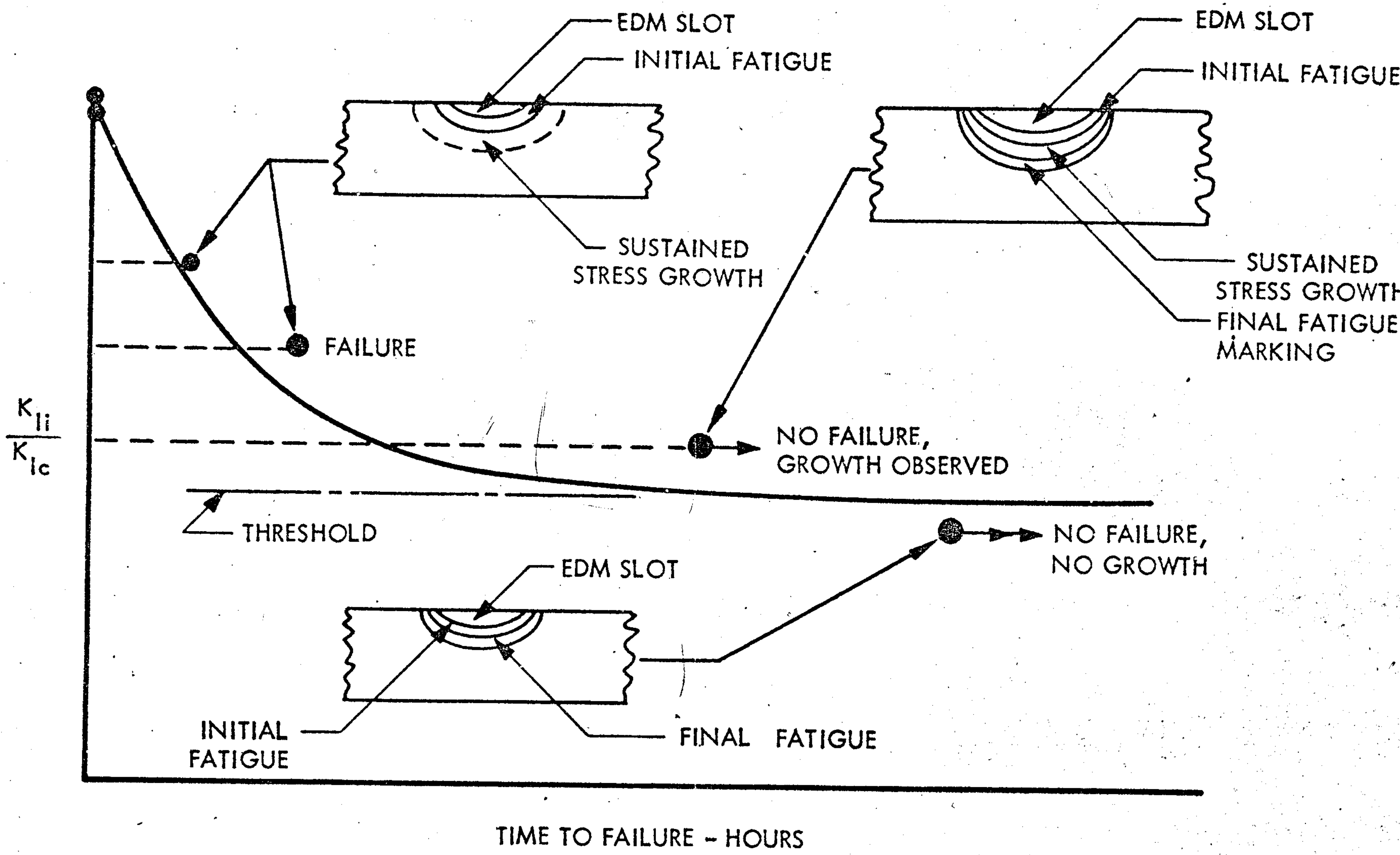

Figure 14: SUSTAINED STRESS FLAW GROWTH TEST APPROACH

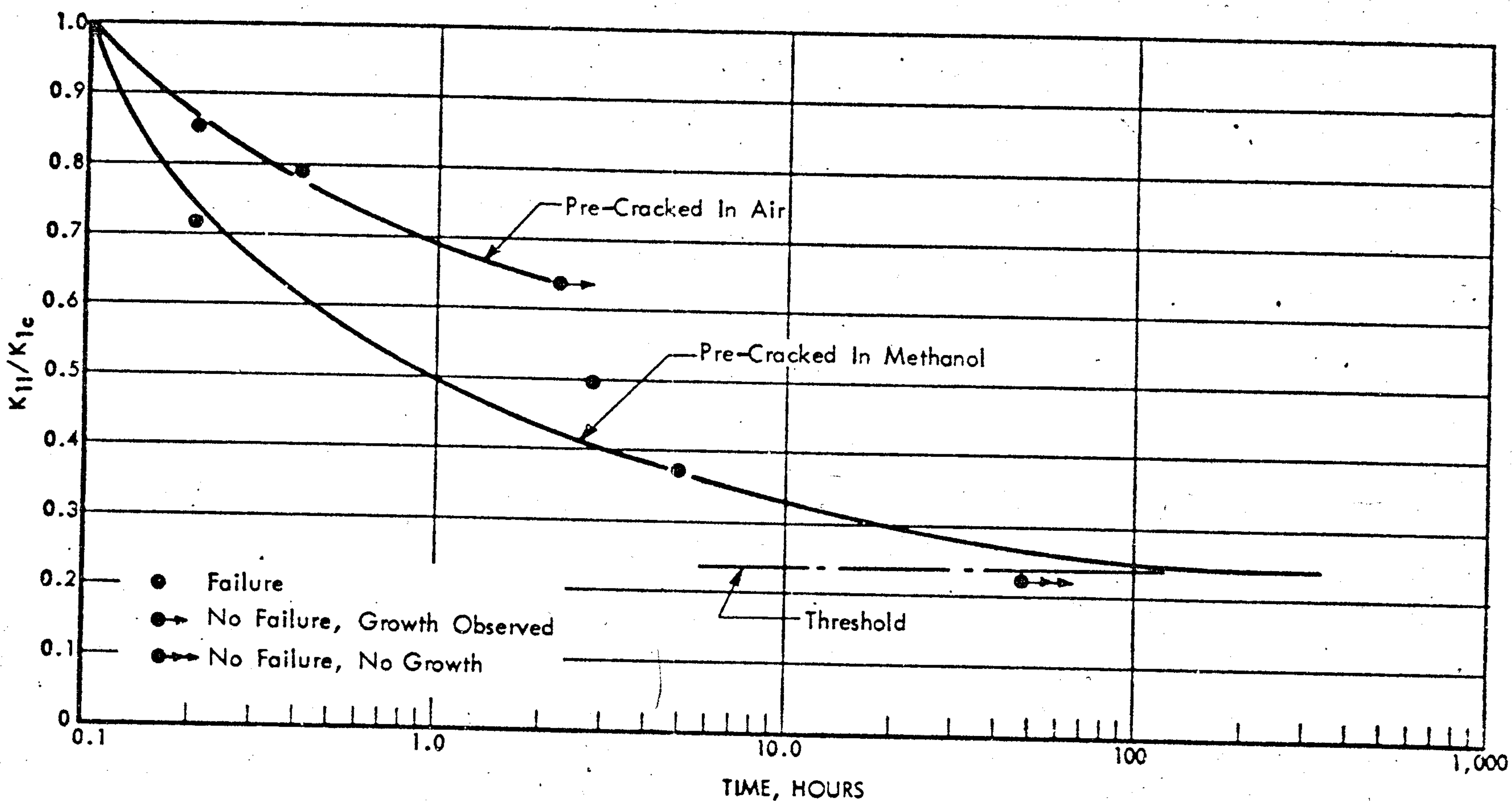

Figure 15 : SUSTAINED LOAD FLAW GROWTH IN METHANOL
(Base Metal At 72 °F)

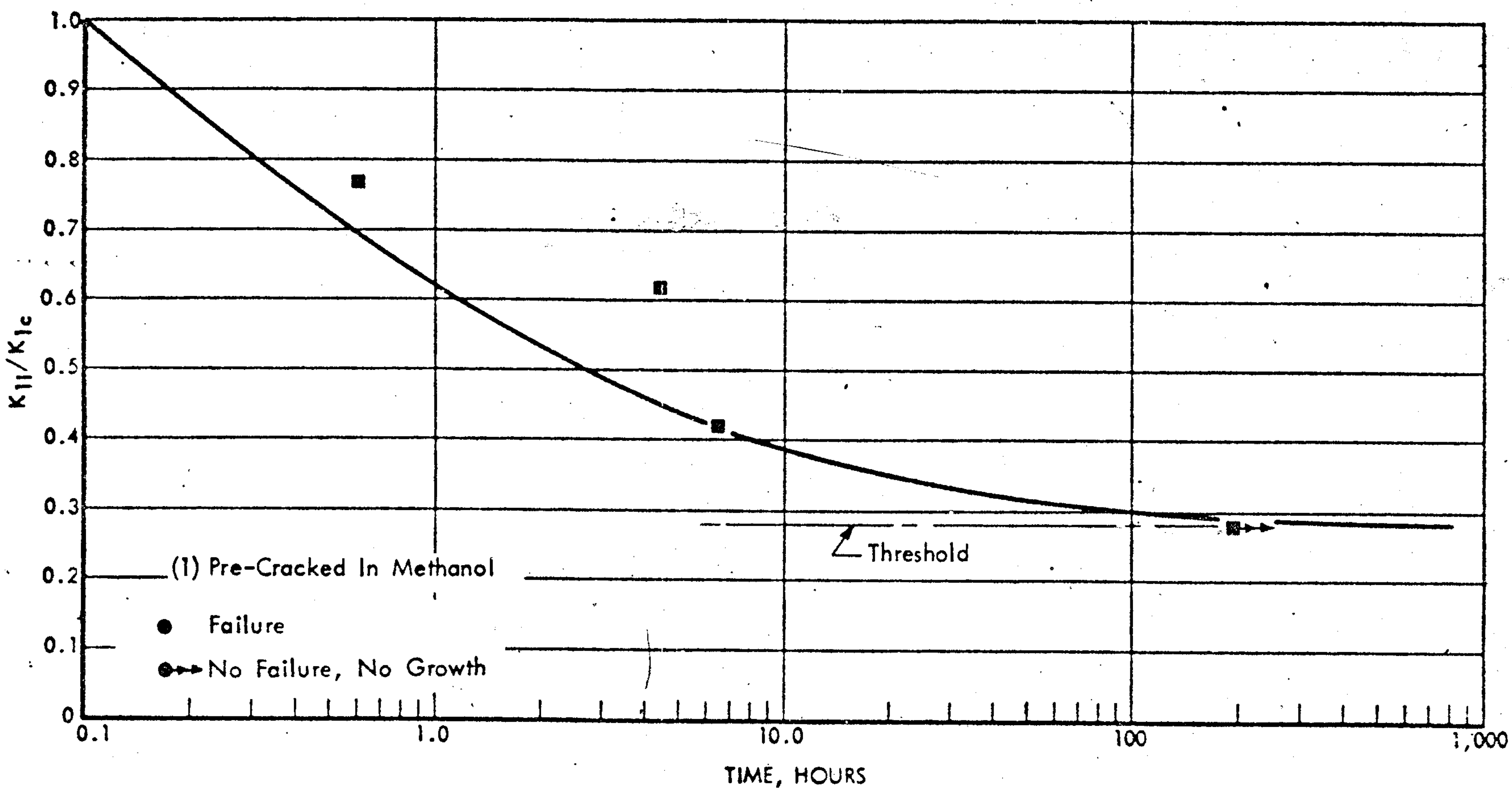

Figure 16: SUSTAINED LOAD FLAW GROWTH IN METHANOL [1]
(Weld H.A.Z. At 72 °F)

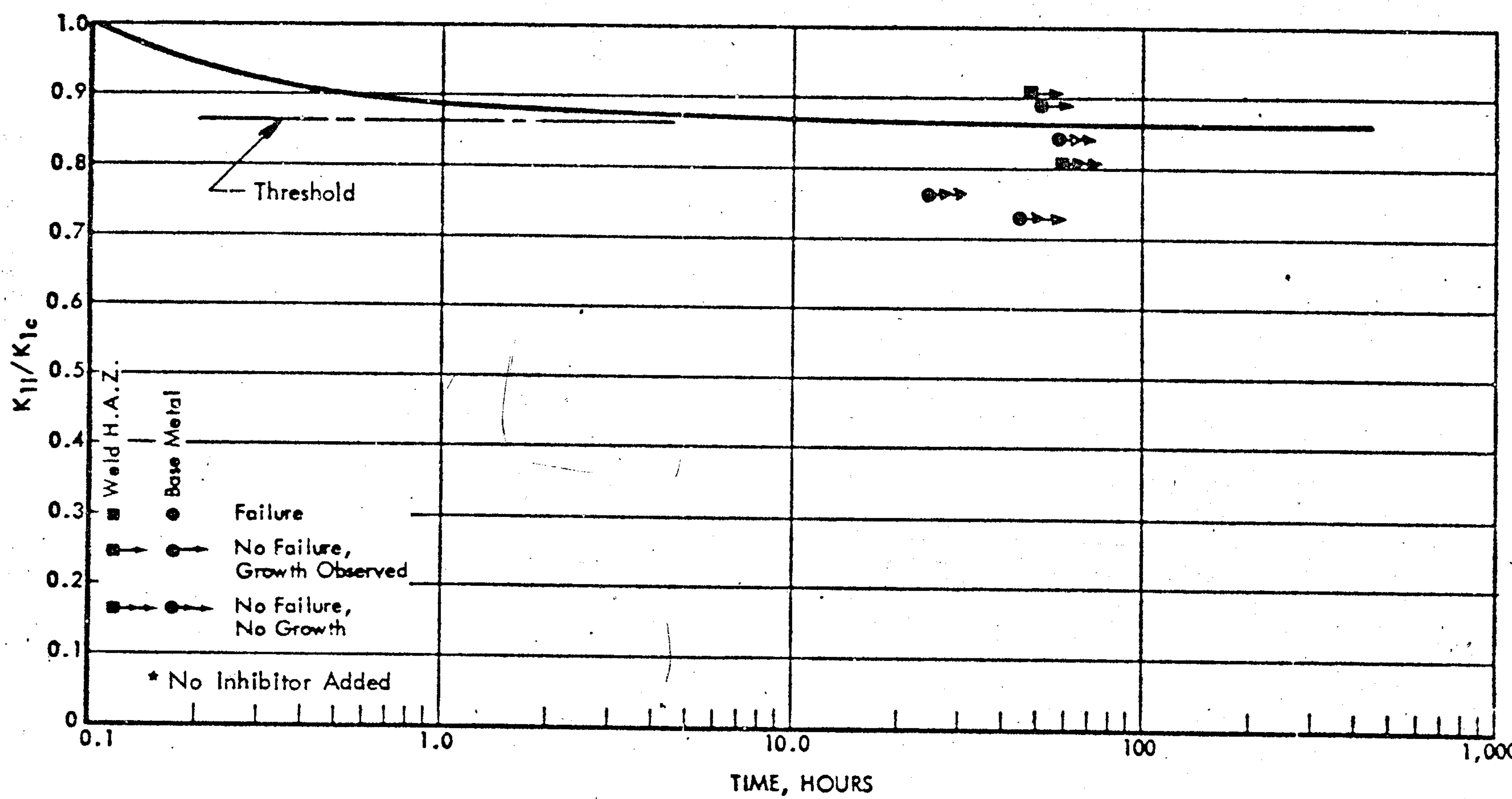

Figure 17: SUSTAINED LOAD FLAW GROWTH IN DISTILLED WATER *
(Base Metal & Weld H.A.Z. At 65 °F)

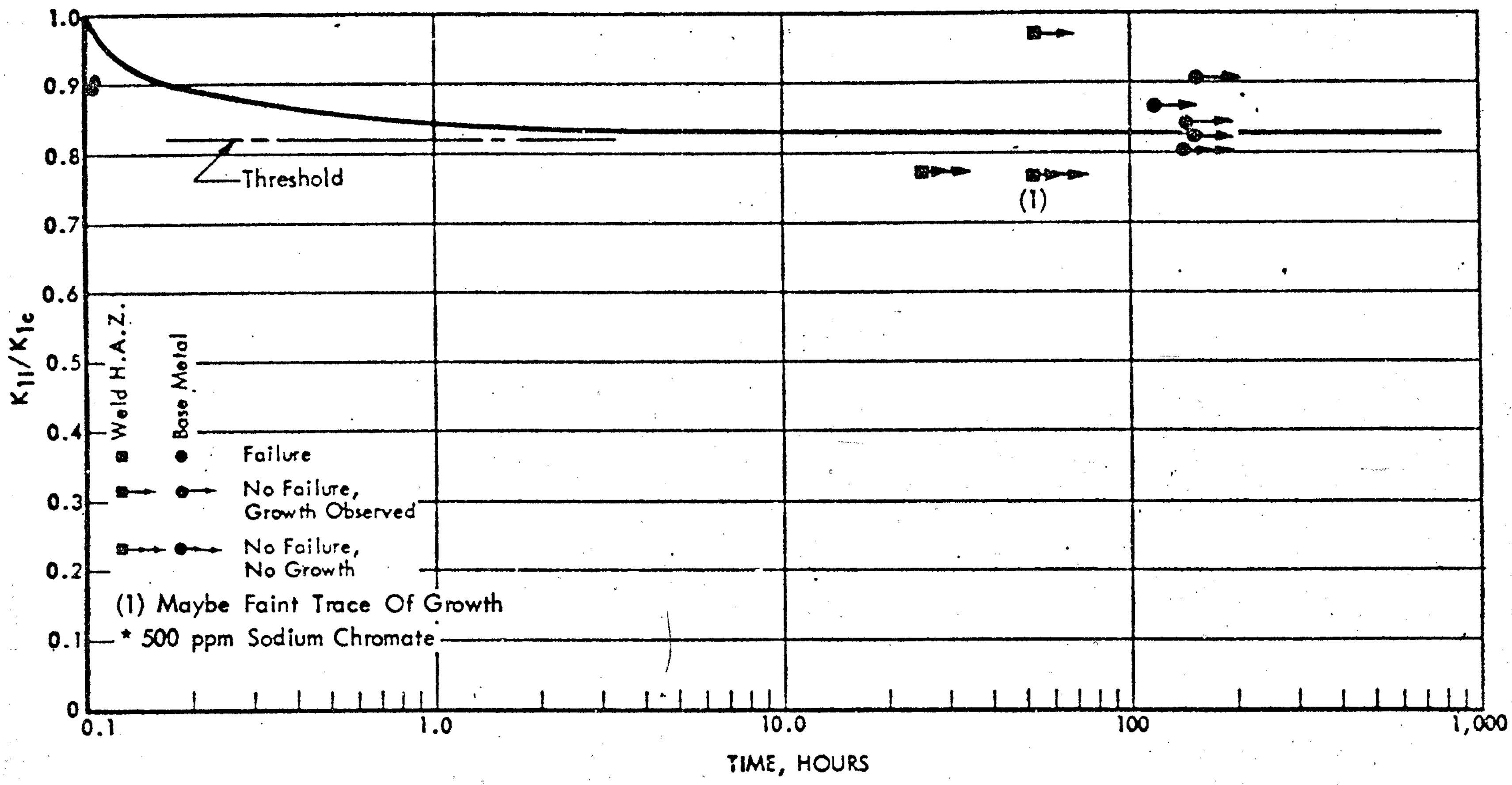

Figure 18: SUSTAINED LOAD FLAW GROWTH IN INHIBITED DISTILLED WATER*
(Base Metal & Weld H. A. Z. At R. T.)

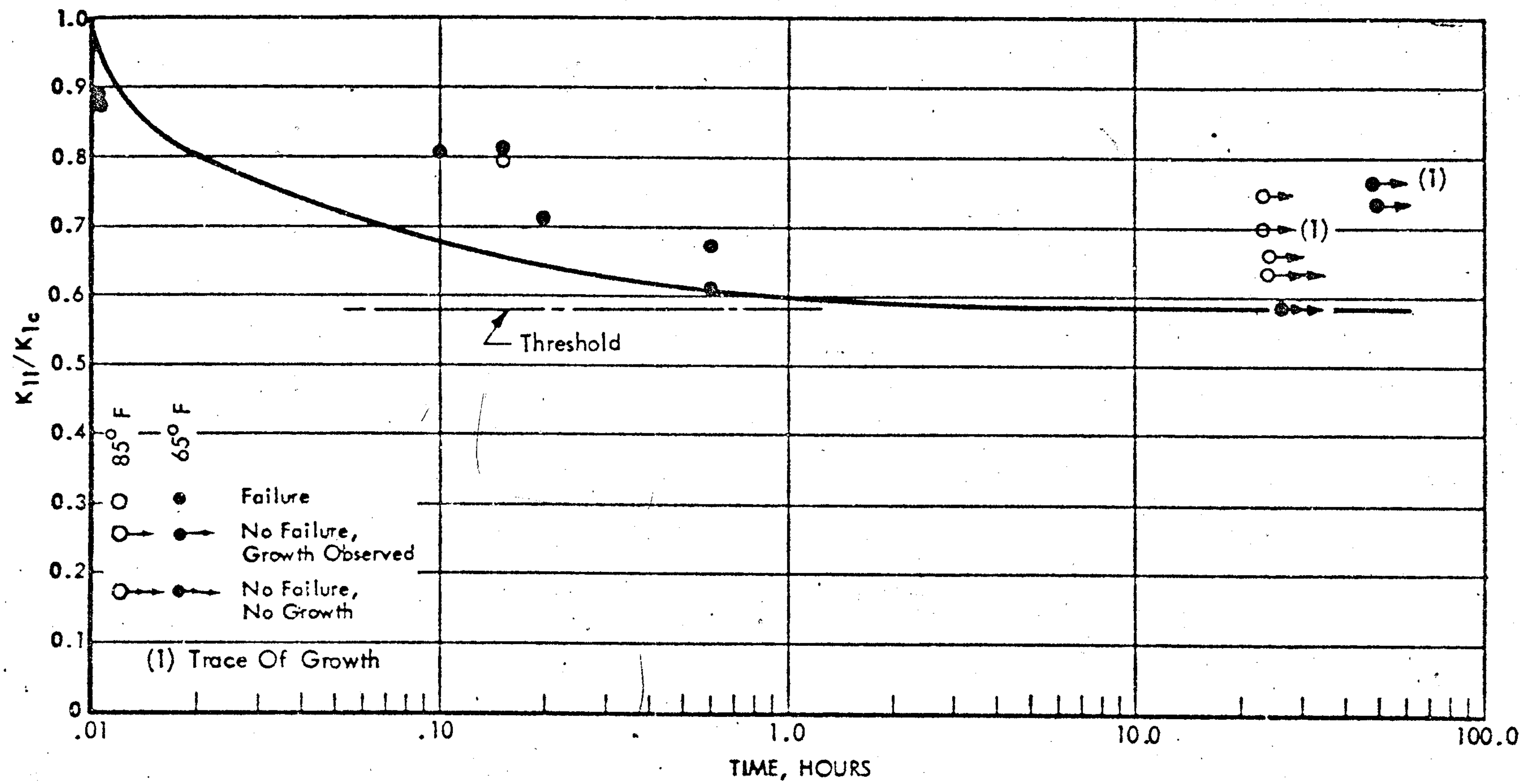

Figure 19 : SUSTAINED LOAD FLAW GROWTH IN FREON MF)
(Base Metal At 65 & 85 °F)

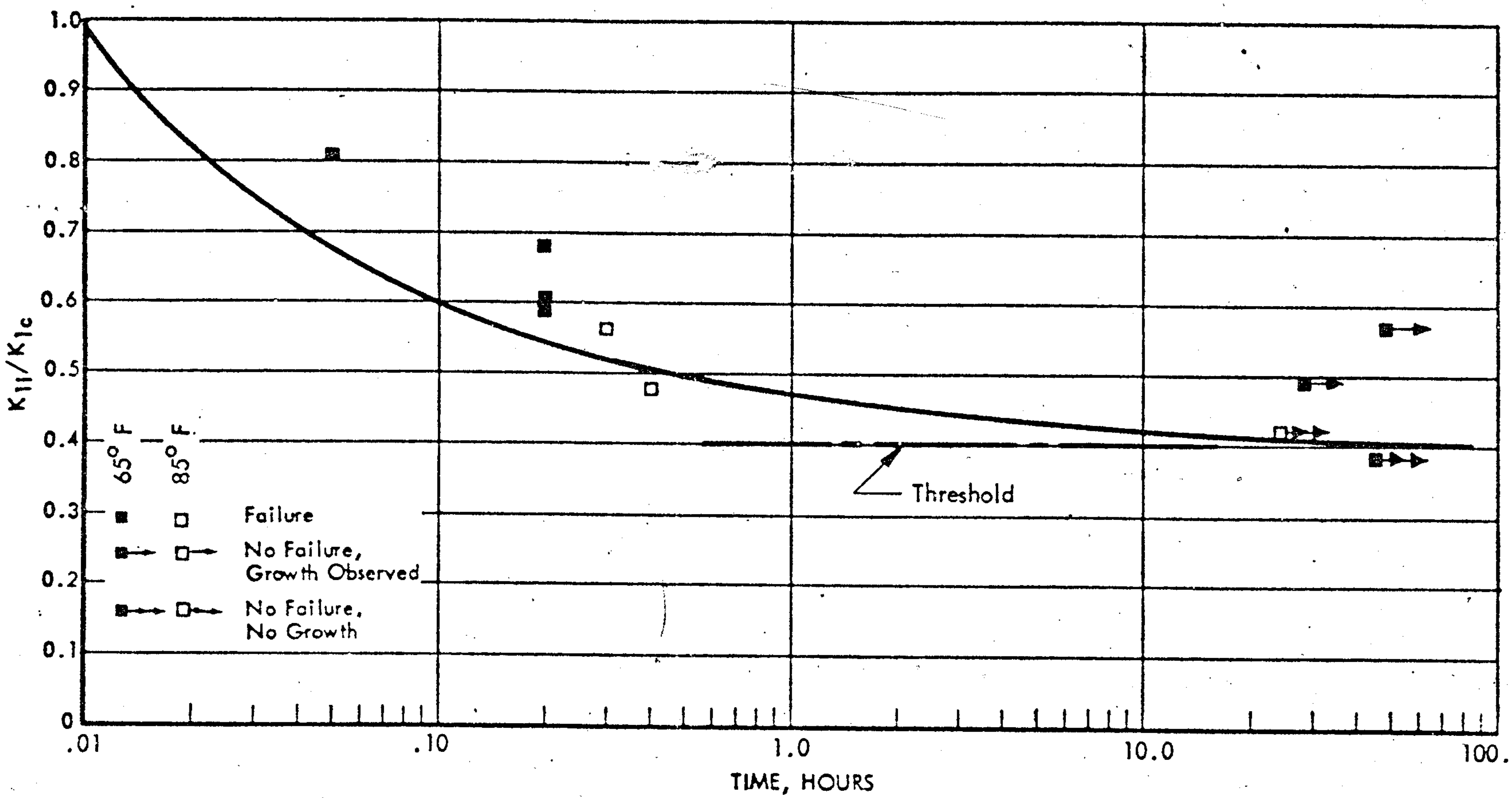

Figure 20: SUSTAINED LOAD FLAW GROWTH IN FREON MF
(Weld H. A. Z. At 65 & 85 °F)

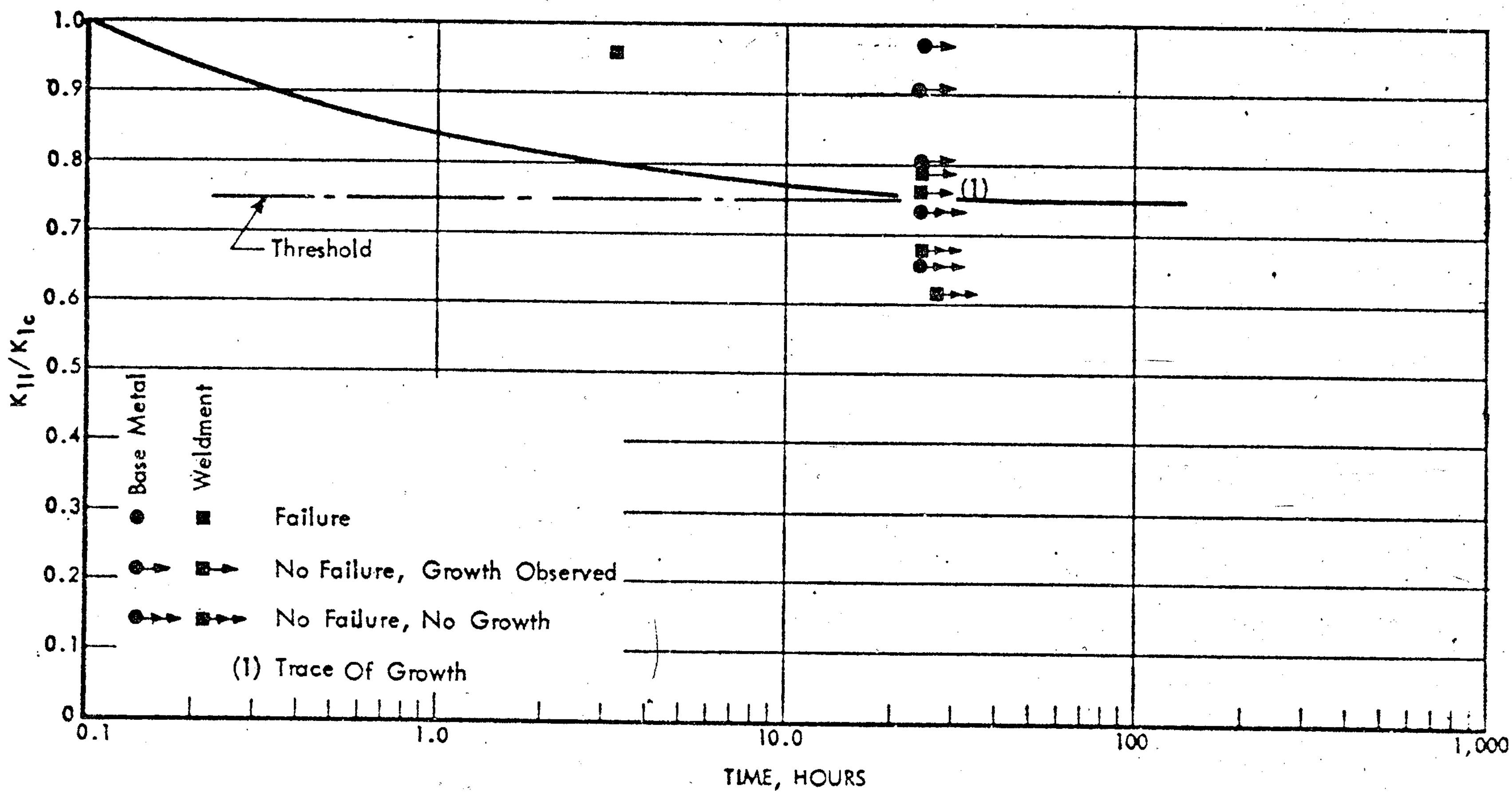

Figure 21: SUSTAINED LOAD FLAW GROWTH IN MONOMETHYLHYDRAZENE
(Base Metal And Weld H. A. Z. At 105 °F)

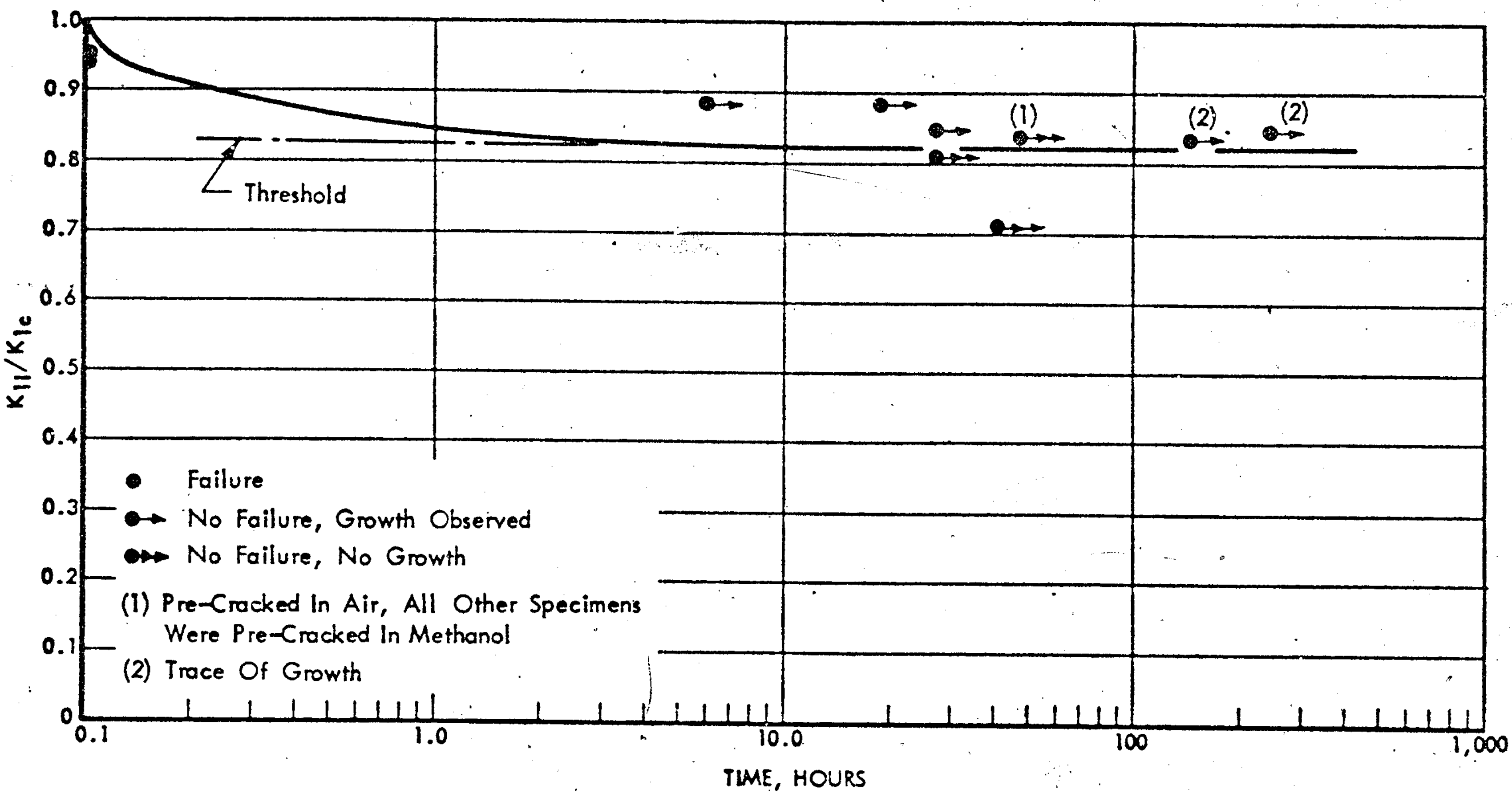

Figure ~~22~~ 1: SUSTAINED LOAD FLAW GROWTH IN AEROZENE 50
(Base Metal At 65 - 79 °F)

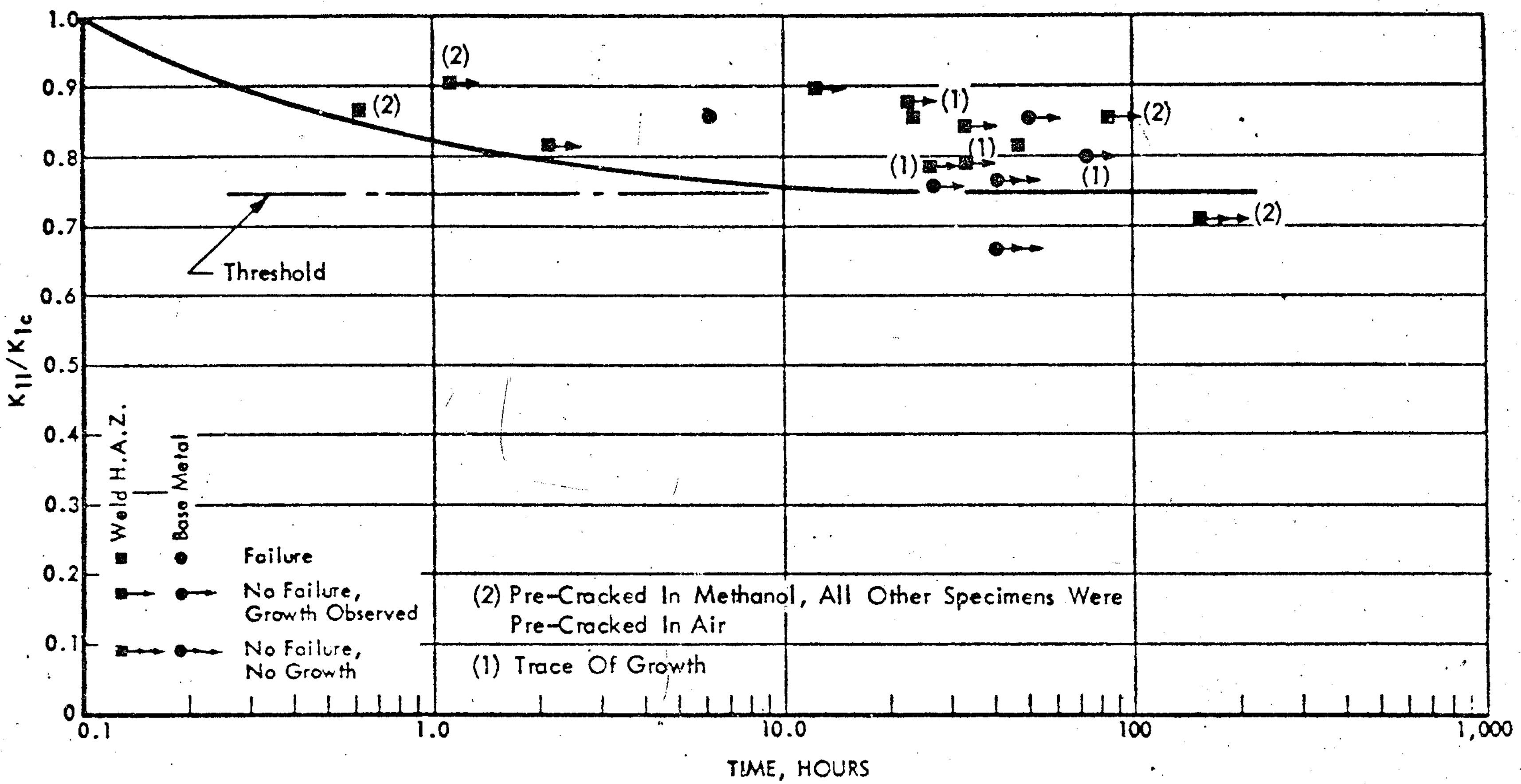

Figure 23: SUSTAINED LOAD FLAW GROWTH IN AEROZENE 50
(Base Metal & Weld H.A.Z. At 110 °F)

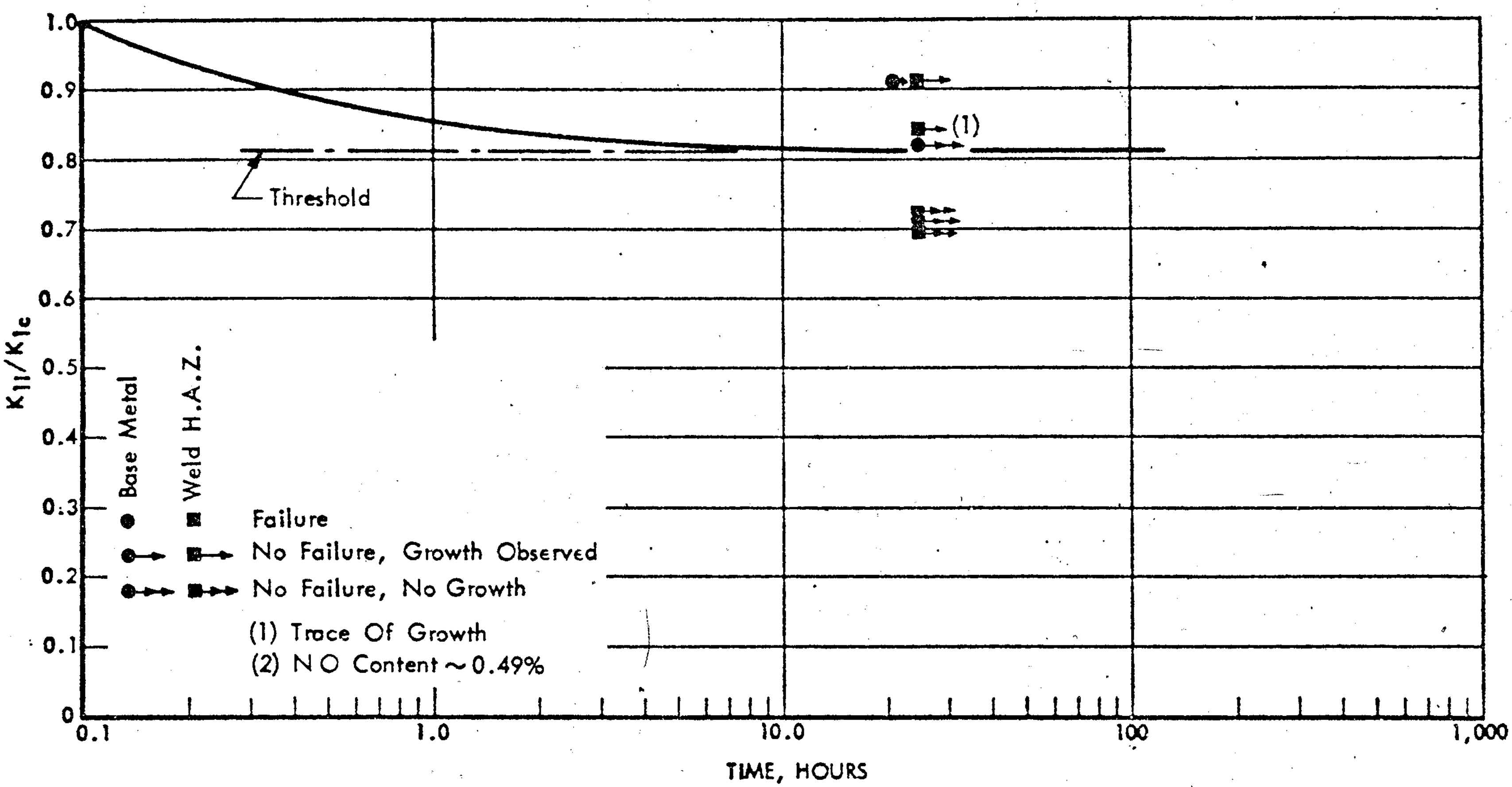

Figure 24: SUSTAINED LOAD FLAW GROWTH IN N_2O_4 (2)
(Base Metal & Weld H.A.Z. At 70 °F)

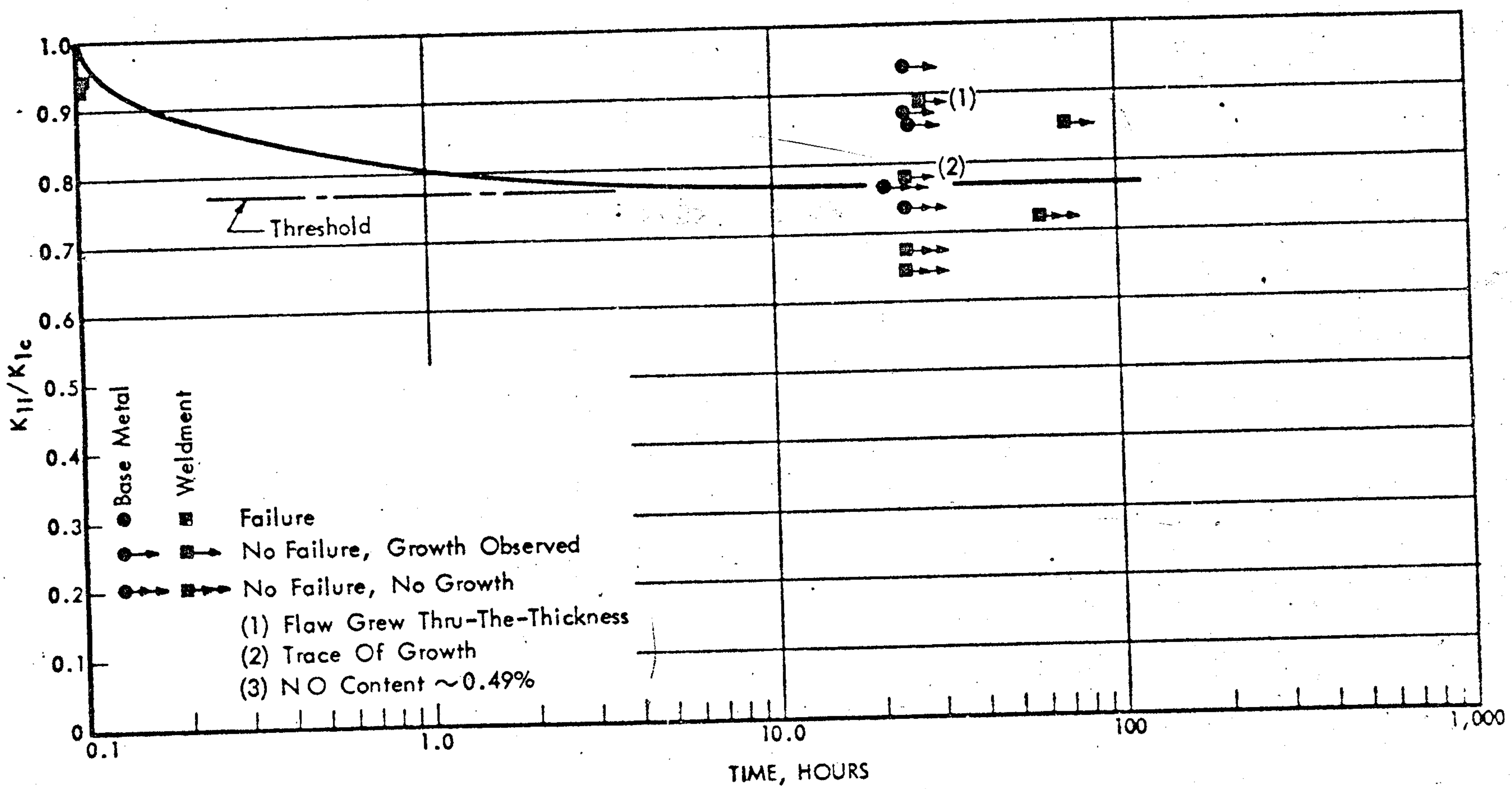

Figure 25: SUSTAINED LOAD FLAW GROWTH IN N_2O_4(3)
(Base Metal & Weld H. A. Z. At 85 ^{o}F)

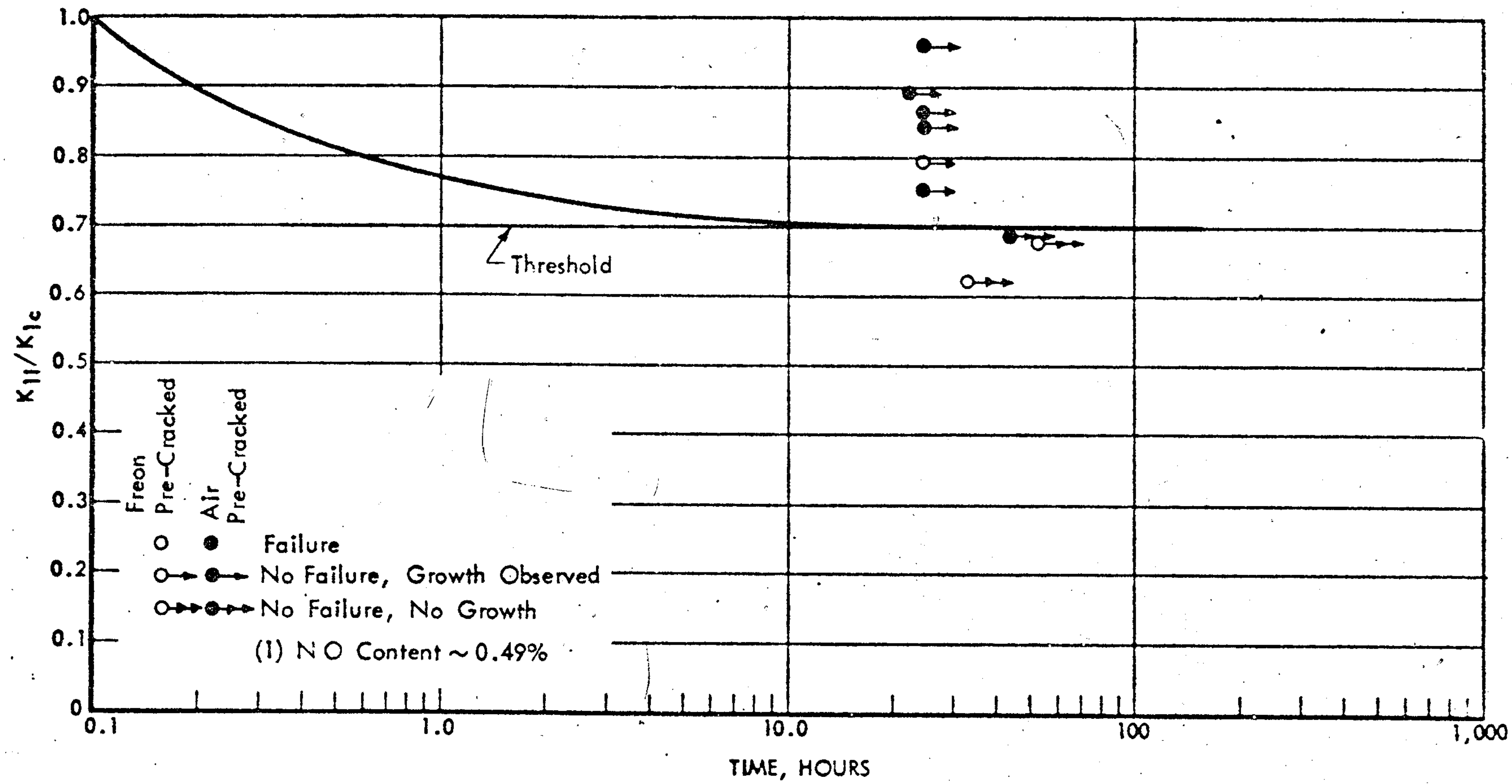

Figure 26: SUSTAINED LOAD FLAW GROWTH IN N_2O_4(1)
(Base Metal At 105 °F)

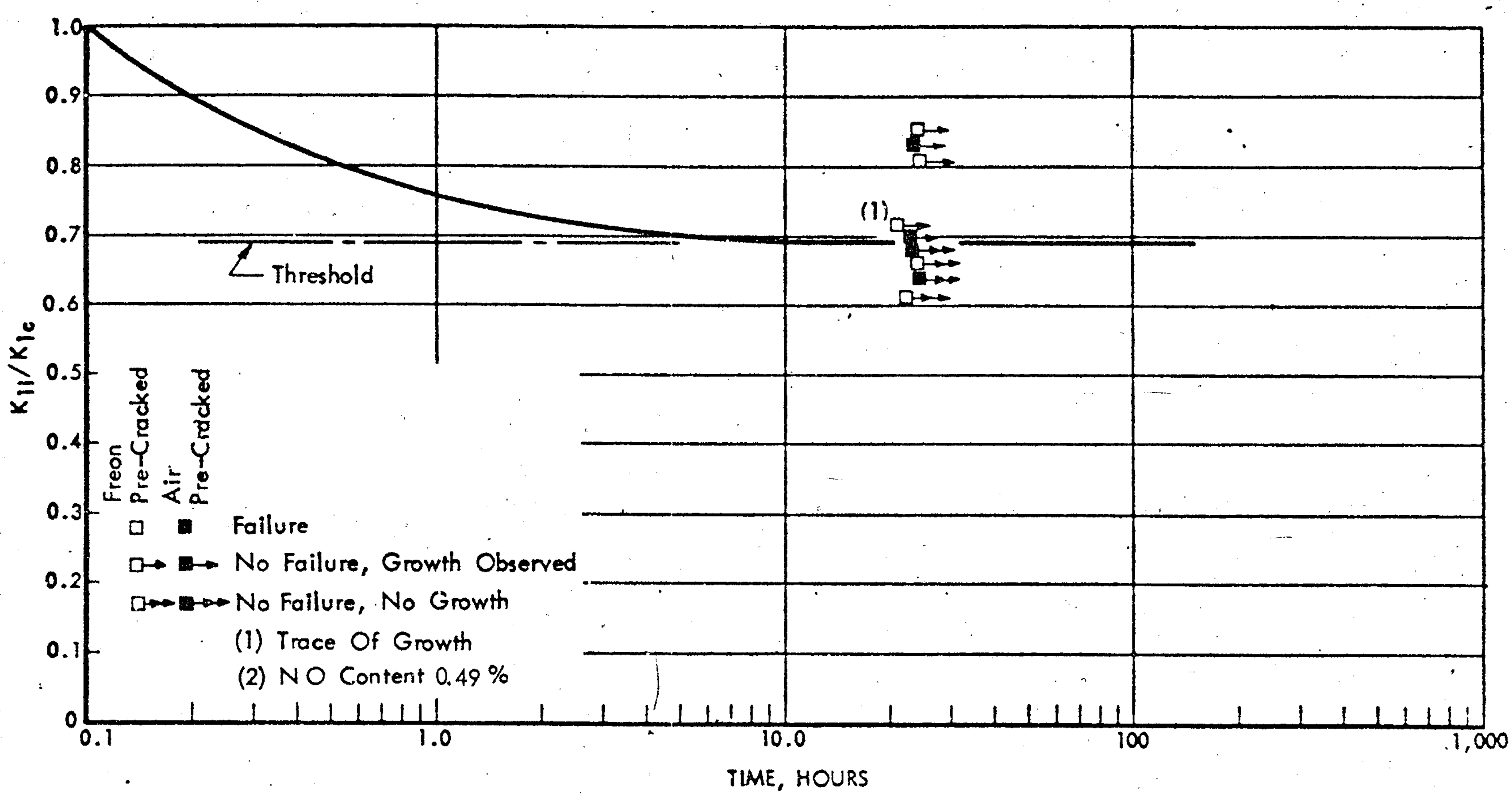

Figure 27: SUSTAINED LOAD FLAW GROWTH IN N_2O_4 [2]
(Weld H. A. Z. At 105 °F)

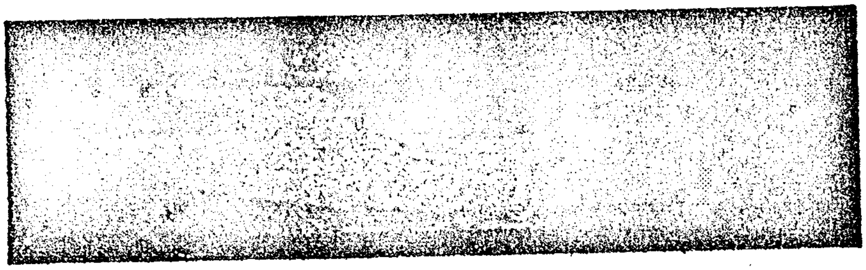

Specimen D-49
$K_{1i}/K_{1c} = 0.969$

Specimen D-50
$K_{1i}/K_{1c} = 0.913$

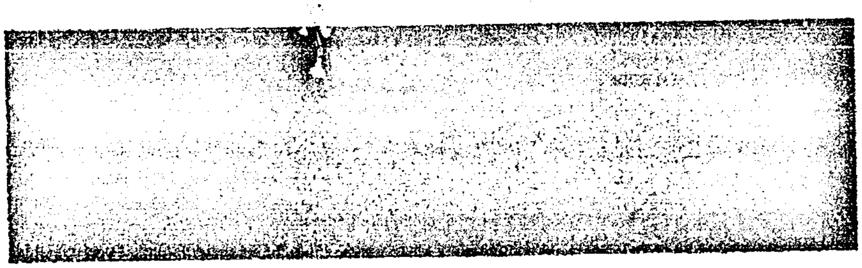

Specimen D-48
$K_{1i}/K_{1c} = 0.806$

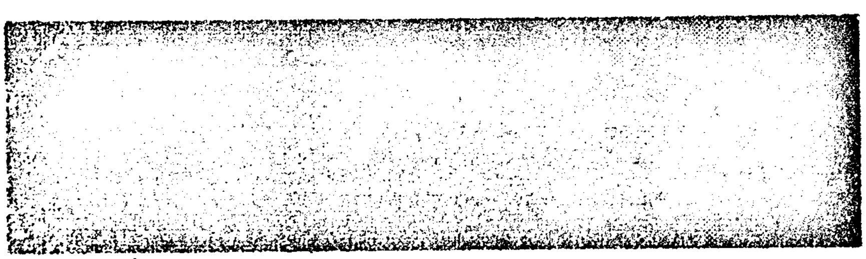

Specimen D-51
$K_{1i}/K_{1c} = 0.731$

Figure 28 : FRACTOGRAPHS OF BASE METAL SPECIMENS
TESTED IN MONOMETHYLHYDRAZENE

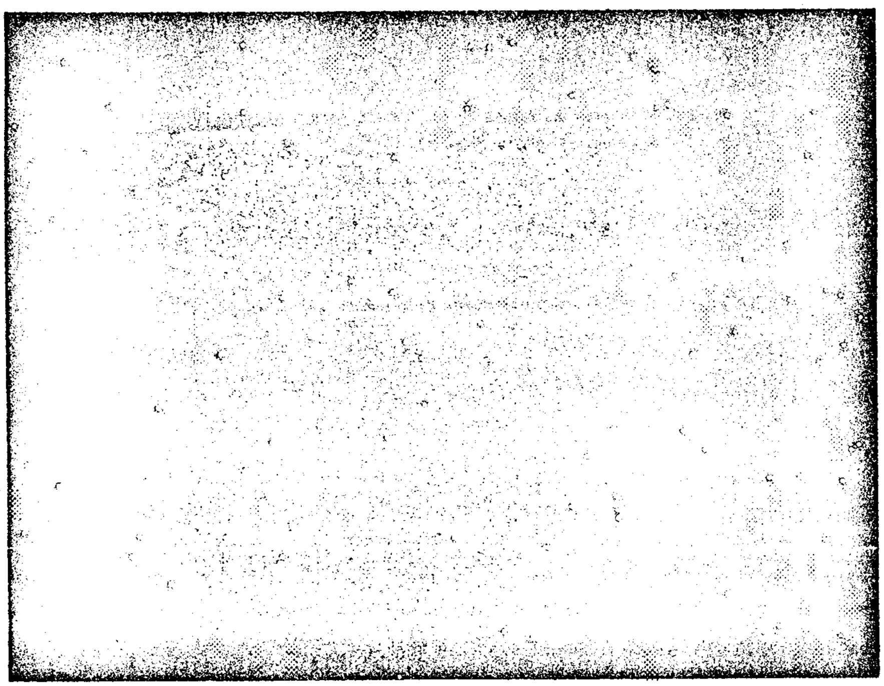

SPECIMEN # 5

BASE METAL (FORGING A)
SUSTAINED LOAD
18.5 HOURS AT
$K_{Ii} = 38.9$ KSI $\sqrt{\text{IN.}}$
IN AEROZENE

Figure 29: FRACTOGRAPH OF BASE METAL SPECIMEN TESTED IN AEROZENE 50

SPECIMEN # 44

BASE METAL (FORGING C)
SUSTAINED LOAD
153.3 HOURS AT
$K_{II} = 41.5$ KSI $\sqrt{\text{IN.}}$
IN INHIBITED WATER

Figure 30 : FRACTOGRAPH OF BASE METAL SPECIMEN TESTED IN INHIBITED WATER

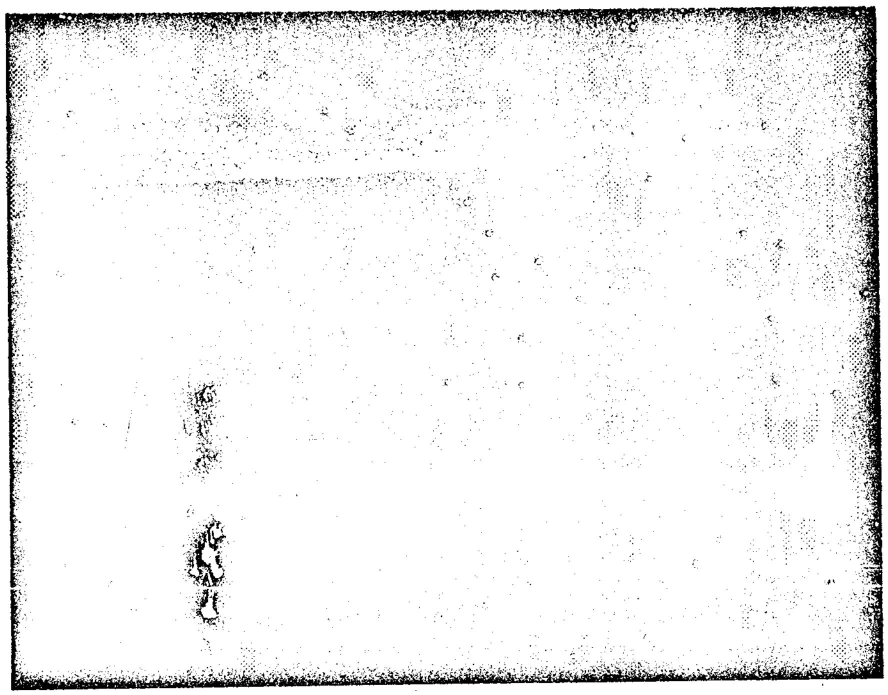

SPECIMEN # W-26
WELDMENT
SUSTAINED LOAD
51.7 HOURS AT
$K_{II} = 38.3$ KSI $\sqrt{\text{IN.}}$
IN INHIBITED WATER

Figure 31: FRACTOGRAPH OF WELD SPECIMEN TESTED IN INHIBITED WATER

SPECIMEN # 14

BASE METAL (FORGING A)

SUSTAINED LOAD

2.2 HOURS AT

$K_{Ii} = 27.6$ KSI $\sqrt{\text{IN.}}$

IN METHANOL

Figure 32: FRACTOGRAPH OF BASE METAL SPECIMEN TESTED IN METHANOL

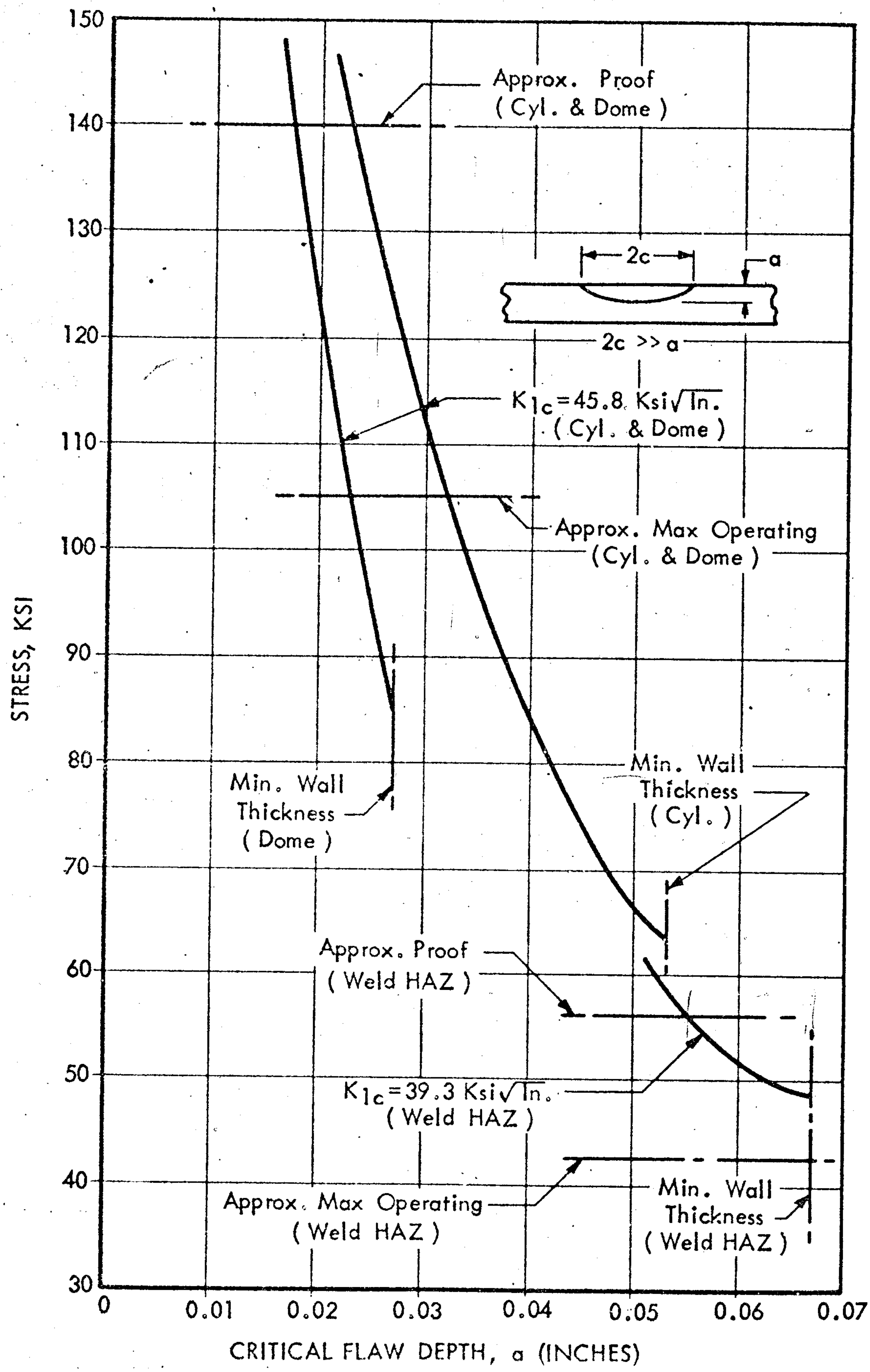

Figure 33: CRITICAL FLAW SIZE CURVES

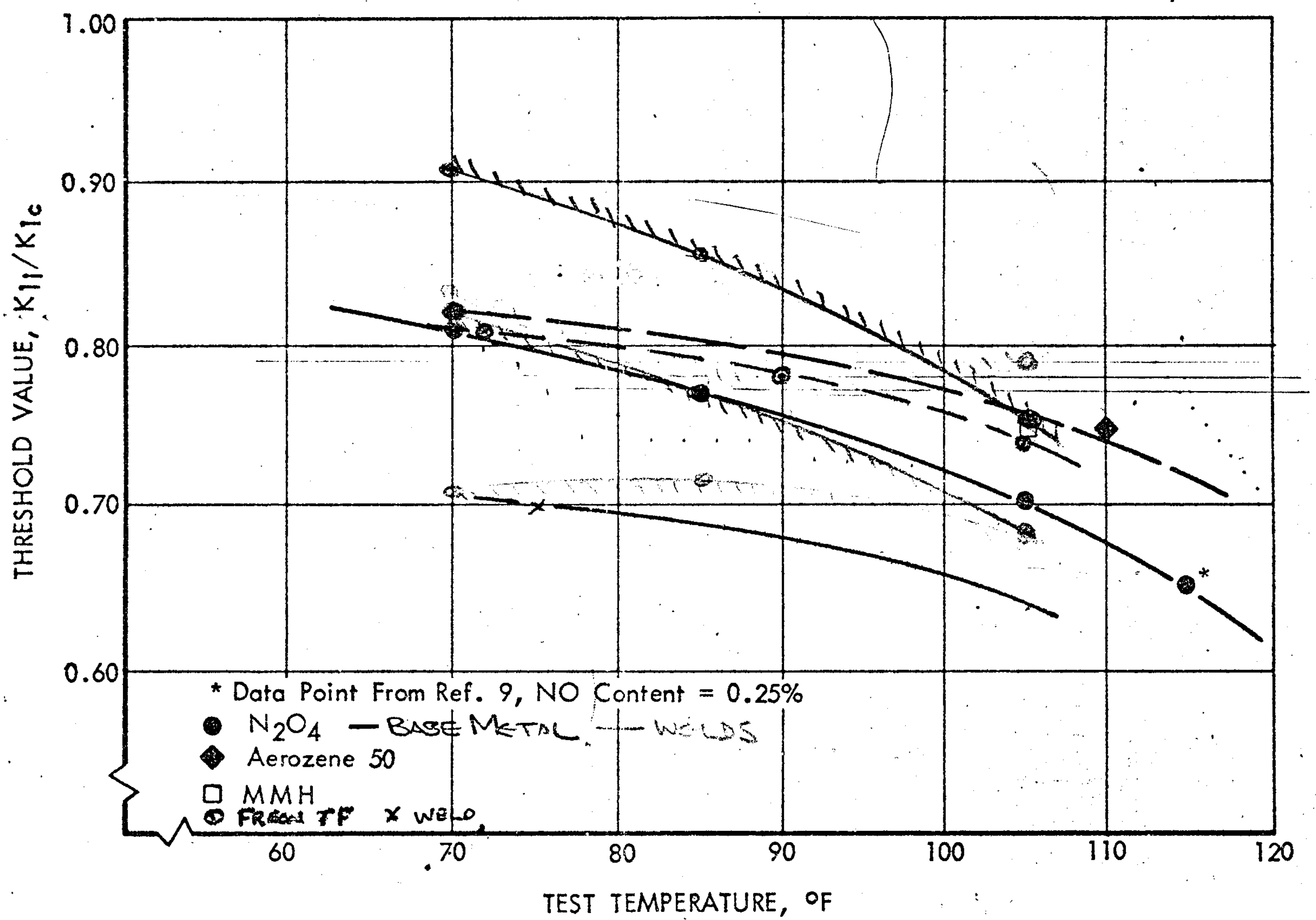

Figure 34 : EFFECT OF TEMPERATURE ON THRESHOLD VALUES

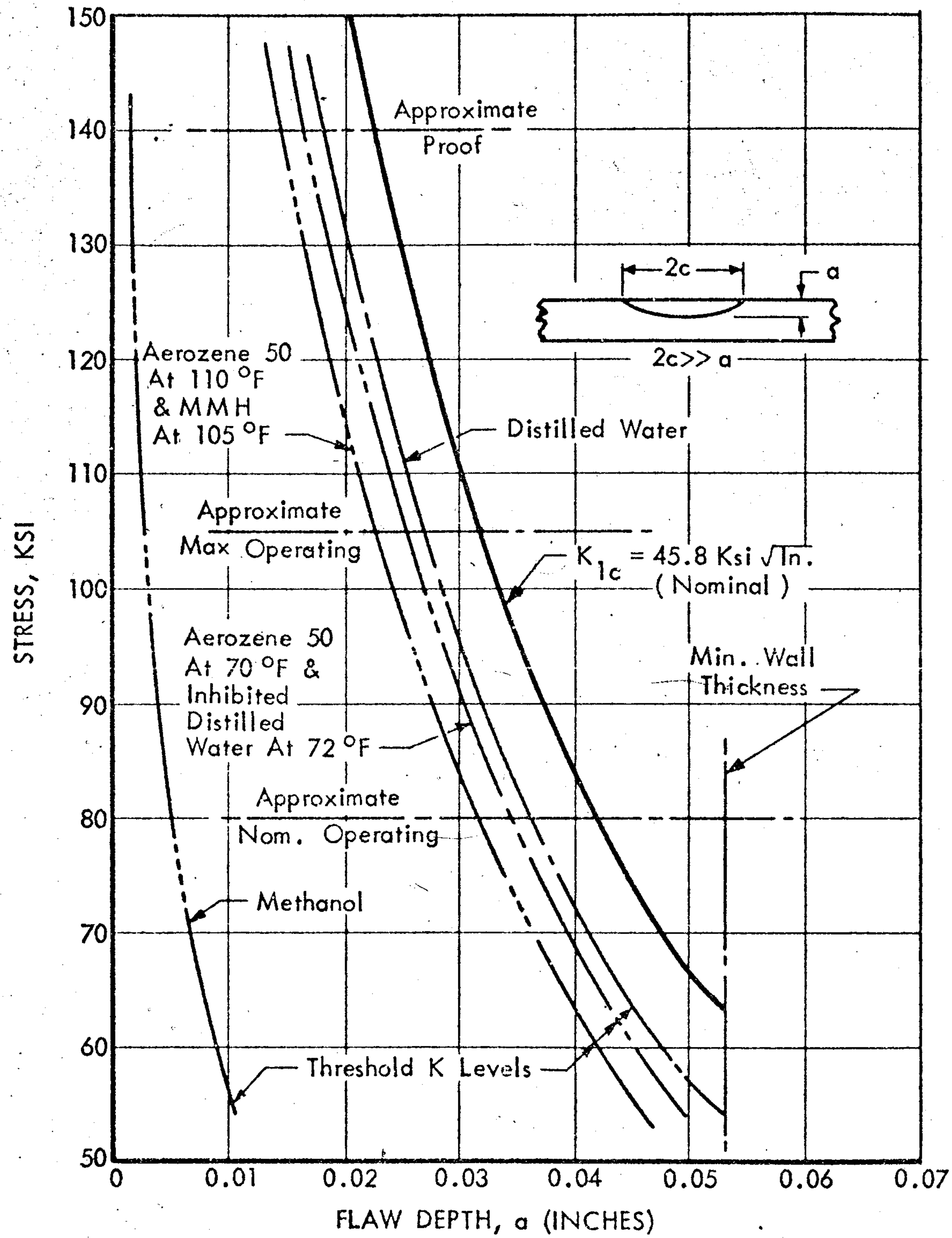

Figure 35: CRITICAL AND THRESHOLD FLAW SIZE CURVES
(S P S Fuel Tank Cylinder)

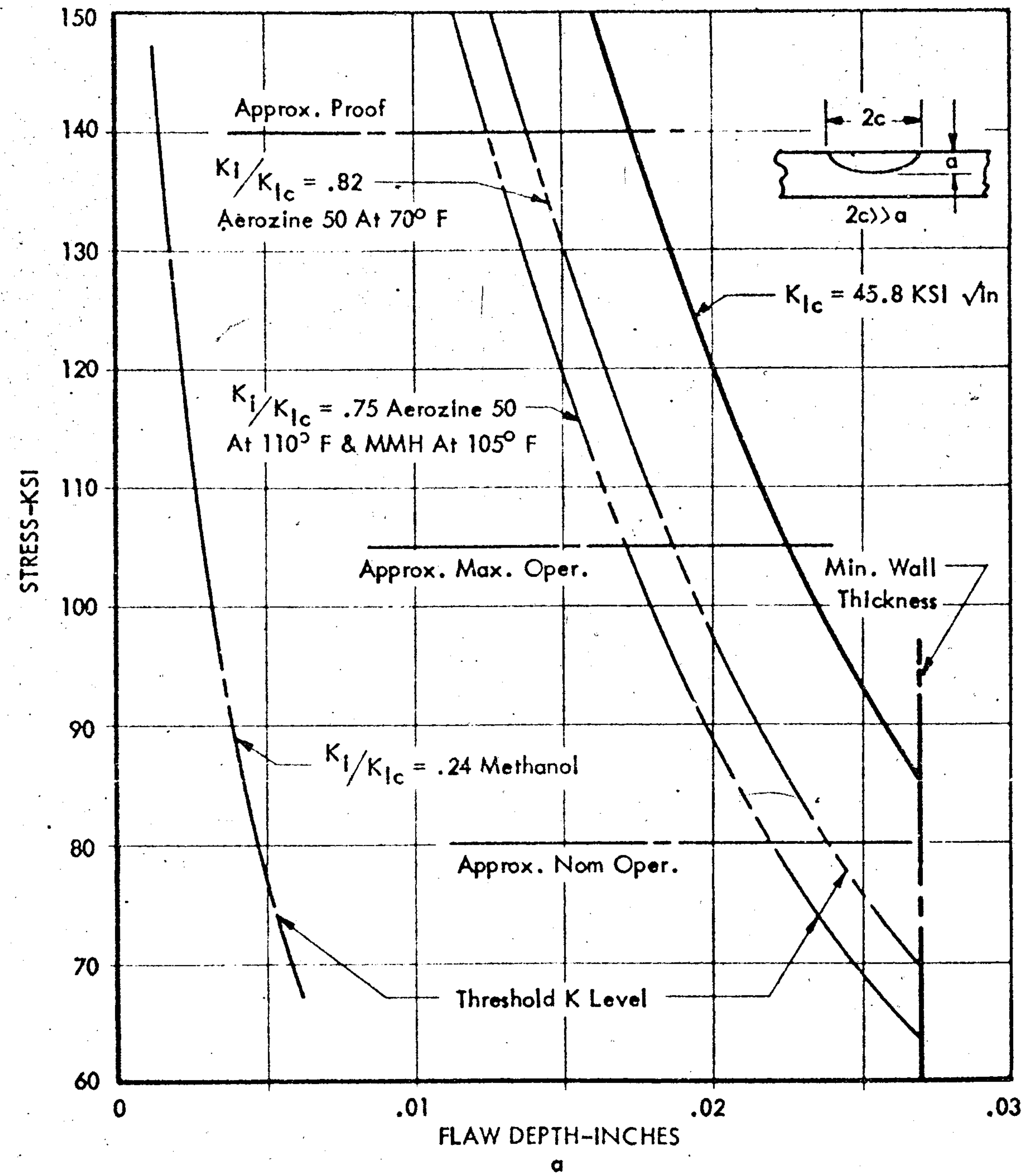

Figure 36: CRITICAL AND THRESHOLD FLAW SIZE CURVES
(S P S Fuel Tank Dome)

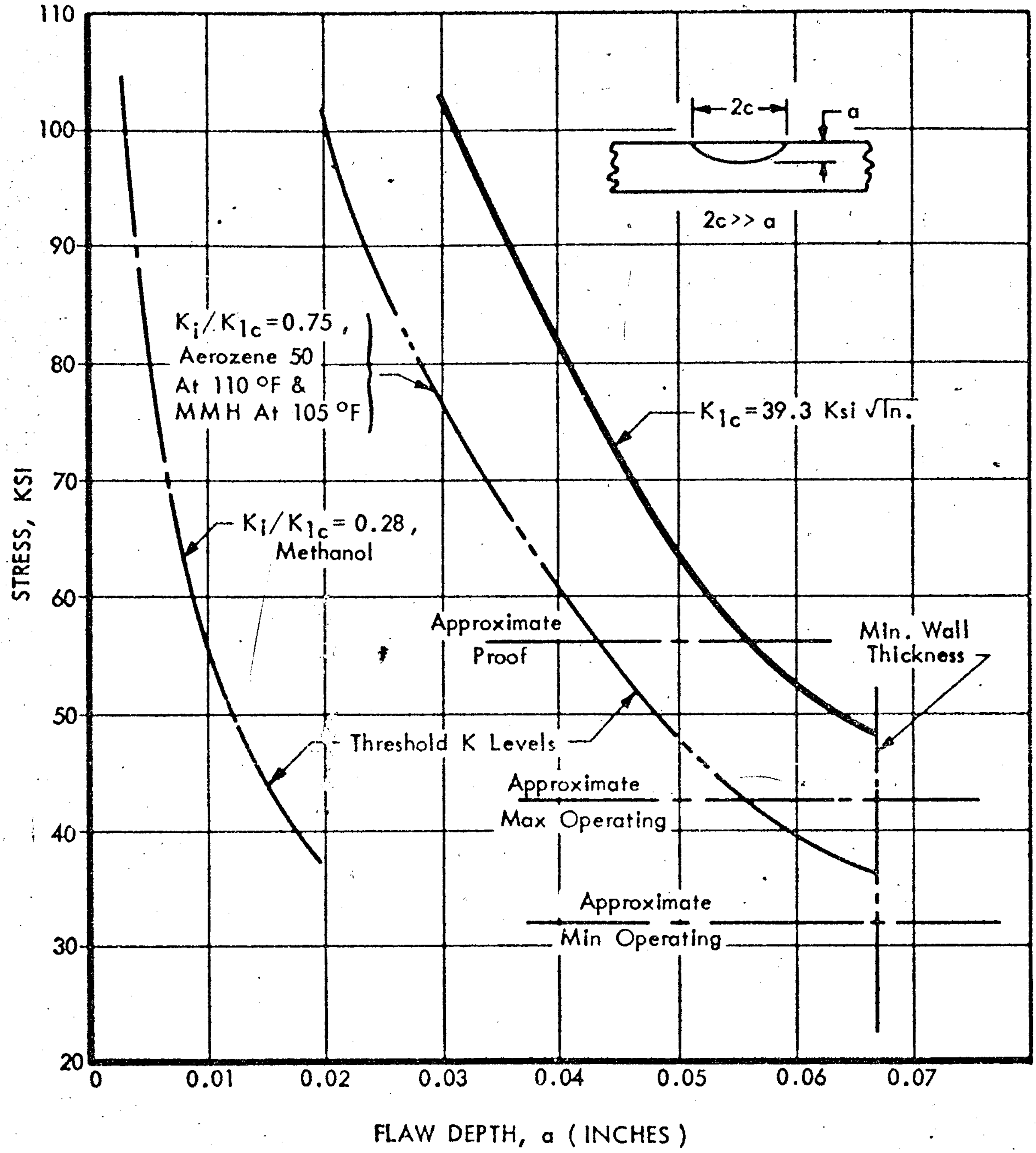

Figure 37: CRITICAL AND THRESHOLD FLAW SIZE CURVES
(S P S Fuel Tank Weldment H. A. Z.)

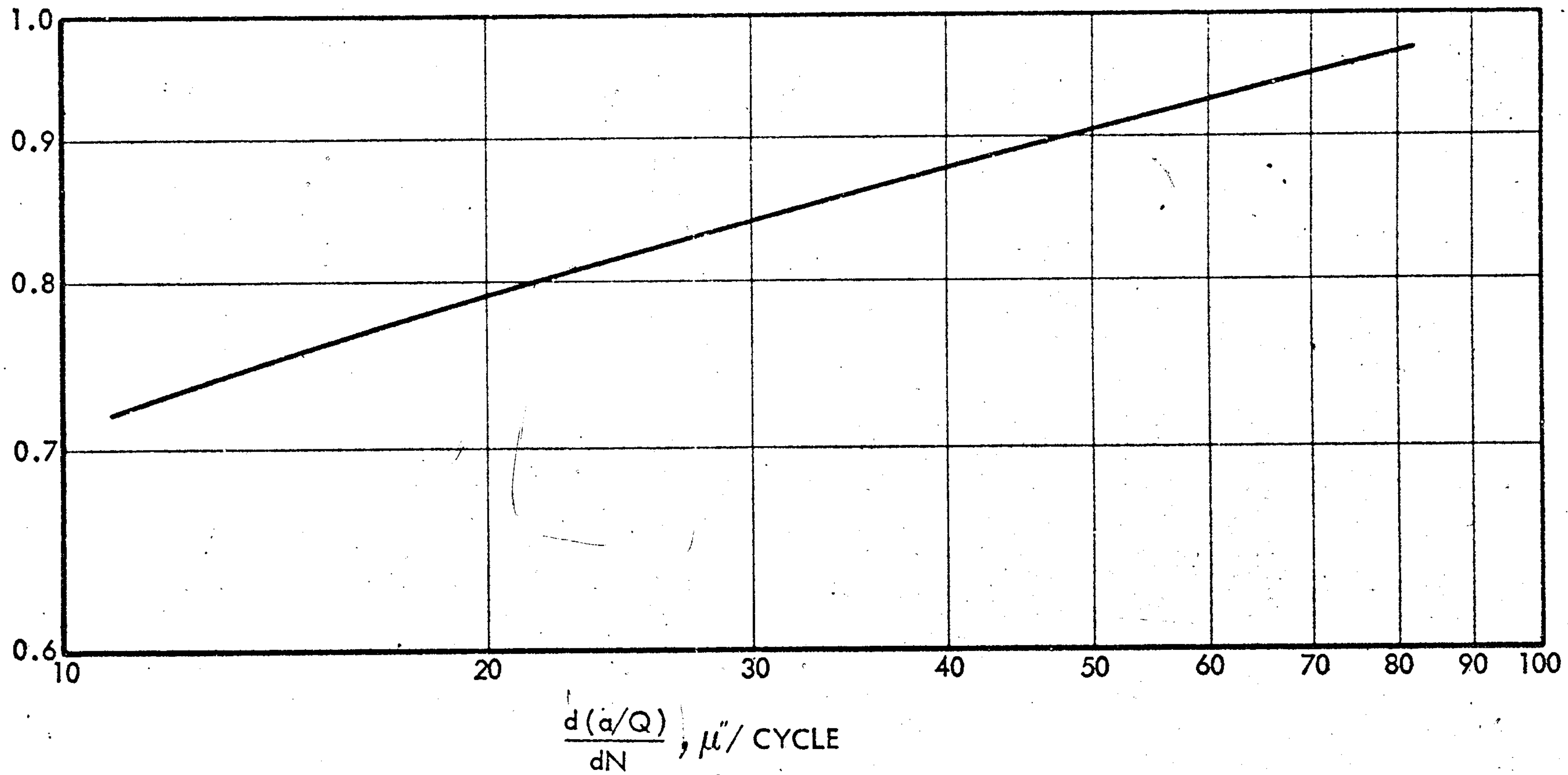

* From 6Al-4V Forgings Cycled In Aerozene, (See Table XXIII) And Converted To Cyclic Stress Of 105 Ksi

Figure 38: CYCLIC FLAW GROWTH RATE*

.00015

DISTRIBUTION LIST FOR FINAL REPORT NASA CR-65586

CONTRACT NAS 9-6665

"INVESTIGATION OF THE FLAW GROWTH CHARACTERISTICS OF 6Al-4V TITANIUM USED IN APOLLO SPACECRAFT PRESSURE VESSELS"

The Boeing Company

		Copies
National Aeronautics and Space Administration Manned Spaceflight Center Houston, Texas, 77058		
Attention:	Contracting Officer, BG 721	1
	S. V. Glorioso, ES4	40
National Aeronautics and Space Administration Washington, D. C. 20546		
Attention:	Code RV-2	1
Scientific and Technical Information Facility P.O. Box 5700 Bethesda, Maryland 20014		
Attention:	NASA Representative Code CRT	1
National Aeronautics and Space Administration Ames Research Center Moffett Field, California 94035		
Attention:	Library	1
National Aeronautics and Space Administration Lewis Research Center 2100 Brookpark Road Cleveland, Ohio 44135		
Attention:	G. T. Smith, MS 49-1	1
	Library	1
	W. F. Brown, MS 105-1	1
	J. L. Shannon, MS 105-1	1
Wright-Patterson Air Force Base, Ohio 45433		
Attention:	AFML(MAAE)	1
Wright-Patterson Air Force Base, Ohio 45433		
Attention:	AFML(MAAM)	1

	Copies
Aerojet-General Corporation P. O. Box 1947 Sacramento, California 95809	
Attention: Technical Library 2484-2015A	1
C. E. Hartbower	1
Douglas Aircraft Company, Inc. Santa Monica Division 3000 Ocean Park Boulevard Santa Monica, California 90405	
Attention: Mr. J. L. Waisman	1
G. V. Bennett, Missiles and Space Systems Division	1
B. V. Whiteson, Missiles & Space Systems Division	1
E. I. dePont deNemours and Company Eastern Laboratory Gibbstown, New Jersey 08027	
Attention: Mrs. Alice R. Steward	1
General Dynamics/Astronautics P.O. Box 1128 San Diego, California 92112	
Attention: Library and Information Services (128-00)	1
General Dynamics/Ft. Worth Ft. Worth, Texas	
Attention: F. C. Nordquist	1
AiResearch Manufacturing Company 9851 Sepulveda Boulevard Los Angeles, 45, California	
Attention: C. M. Campbell	1
National Aeronautics and Space Administration NASA/Headquarters Washington, D. C. 20546	
Attention: George Deutch	1
Wright-Patterson Air Force Base, Ohio 45433	
Attention: Howard Zoeller, AFML	1
Capt. N. Tupper, AFML	1
RPMCH/ Edwards, California 93523	
Attention: William Payne	1
RPRPT/ Edwards, California 93523	
Attention: John Branigan	1

Copies

Battelle Memorial Institute	
505 King Avenue	
Columbus, Ohio 43201	
Attention: Report Library, Room 6A	1
G. T. Hahn	1
North American Aviation, Inc.	
Space and Information Systems Division	
12214 Lakewood Boulevard	
Downey, California 90242	
Attention: Technical Information Center	
D/096-722 (AJ01)	1
L. J. Korb	1
R. P. Olsen	1
Rocketdyne	
6633 Canoga Avenue	
Canoga Park, California 91304	
Attention: Library, Department 596-306	1
W. T. Chandler	1
Martin-Marietta Corporation	
Denver Division, G 0438	
Denver, Colorado 80201	
Attention: F. R. Schwartzberg	1
R. D. Masteller	1
General Dynamics/Convair	
San Diego, California	
Attention: W. E. Witzel, Materials Research Group	2
J. Christian, M. S. 572-10	1